Hindawi
Mathematical Problems in Engineering
Volume 2020, Article ID 2127374, 21 pages
https://doi.org/10.1155/2020/2127374

Research Article

An Improved Hilbert Spectral Representation Method for Synthesizing Spatially Correlated Earthquake Ground Motions and Its Error Assessment

Luhua Zhu[1] and Erlei Yao[1,2]

[1]*School of Civil Engineering and Mechanics, Huazhong University of Science and Technology, Wuhan 430074, China*
[2]*Changjiang River Scientific Research Institute, Wuhan 430010, China*

Correspondence should be addressed to Erlei Yao; xiaoleiip@163.com

Received 26 February 2020; Accepted 5 May 2020; Published 16 May 2020

Guest Editor: Zhimin Zhang

This paper is an extension of the random amplitude-based improved Hilbert spectral representation method (IHSRM) that the authors developed previously for the simulation of spatially correlated earthquake ground motions (SCEGMs) possessing the nonstationary characteristics of the natural earthquake record. In fact, depending on the fundamental types (random phase method and random amplitude method) and matrix decomposition methods (Cholesky decomposition, root decomposition, and eigendecomposition), the IHSRM possesses various types. To evaluate the influence of different types of this method on the statistic errors, i.e., bias errors and stochastic errors, an error assessment for this method was conducted. First, the random phase-based IHSRM was derived, and its reliability was proven by theoretical deduction. Unified formulas were given for random phase- and random amplitude-based IHSRMs, respectively. Then, the closed-form solutions of statistic errors of simulated seismic motions were derived. The validness of the proposed closed-form solutions was proven by comparing the closed-form solutions with estimated values. At last, the stochastic errors of covariance (i.e., variance and cross-covariance) for different types of IHSRMs were compared, and the results showed that (1) the proposed IHSRM is not ergodic; (2) the random amplitude-based IHSRMs possessed higher stochastic errors of covariance than the random phase-based IHSRMs; and (3) the value of the stochastic error of covariance for the random phase-based IHSRM is dependent on the matrix decomposition method, while that for the random amplitude-based one is not.

1. Introduction

The spectral representation method (SRM) proposed by Rice [1] and then extended by Shinozuka and Jan [2–4] is the most widely used method to simulate random processes due to its accuracy and being easy to application [5, 6]. However, the random processes simulated by SRM are not always ergodic; in other words, the temporal statistics estimated from one SRM-simulated sample may be different from the targets [7]. The differences are errors. Besides, to reduce the calculation time and cost involved in the time-history analysis of complex or extended structures, only few samples or a set of random processes (e.g., seismic ground motion) would be generated and used in practice. Because the generated realizations that are utilized as inputs in time domain analysis of structures have great influence on the results [8–12], the rational estimation of these errors is necessary.

The difference between the estimated statistics and the target can be evaluated by the bias and stochastic errors. Hu et al. [13] assessed the errors produced by both the Cholesky decomposition-based SRM and the eigendecomposition-based SRM and found that the latter one produced smaller stochastic errors. Gao et al. [14] compared the bias errors and the stochastic errors of the random process simulated by the random amplitude-based SRM with those by the random phase-based SRM. Gao et al. [7] systematically investigated the bias errors and stochastic errors of the random process

simulated by the coherency matrix-based SRM and compared them with the errors of the PSD matrix-based SRM. Hu et al. [15, 16] studied the statistical errors in the simulation of spatially varying seismic ground motions modeled by evolutionary Gaussian vector processes and simulated by the SRM. They indicated that the SRM implementation scheme involving both random amplitudes and phase angles would cause larger stochastic errors. Wu et al. [17] conducted the error assessment of multivariate random processes simulated by a conditional simulation method.

In accordance with the Hilbert spectral representation model proposed by Wen and Gu [18] and the Hilbert–Huang transform (HHT) [19], the authors had developed a random amplitude-based IHSRM [20] to simulate SCEGMs having natural nonstationary characteristics. To optimize and supplement the IHSRM aforementioned, the random phase-based IHSRM was developed in this paper. More importantly, a series of deduction around the random phase-based IHSRM was then conducted to verify the reliability of this method. Then, considering the fundamental types (random phase method and random amplitude method) and different matrix decomposition methods (Cholesky decomposition, root decomposition, and eigendecomposition) that may be used in the IHSRM, an error assessment was conducted to evaluate the temporal statistic errors of the IHSRM-simulated process. The unified formulas for random phase- and random amplitude-based IHSRMs were presented. Two types of statistical errors were prescribed, and then the closed-form solutions of statistical errors of seismic motions simulated by different types of IHSRMs were derived. The validness of the proposed closed-form solutions was verified by numerical examples. At last but not the least important, the optimal form of IHSRM was found.

2. Theoretical Background

2.1. The Hilbert Spectral Representation Model. A time series can be decomposed into a few intrinsic mode functions (IMFs) using HHT. The extraction of IMFs from a time series entails a repeated "sifting" procedure called empirical mode decomposition (EMD) [19]. After EMD, the original time series $X(t)$ can be expressed in terms of IMFs as follows:

$$X(t) = \sum_{j=1}^{N} I_j(t) + r(t), \tag{1}$$

where N is the number of the IMFs, $I_j(t)$ denotes the jth IMF, and $r(t)$ indicates the residual function. In general, $r(t)$ is too small to be of any consequence, or it becomes a monotonic function from which no IMF can be extracted anymore. Performing the Hilbert transform on $I_j(t)$ yields

$$Q_j(t) = H\left[I_j(t)\right] = \frac{1}{\pi} P \int_{-\infty}^{\infty} \frac{I_j(\tau)}{t-\tau} \mathrm{d}\tau, \tag{2}$$

where P denotes the Cauchy principal value. An analytical function can be formulated as follows:

$$Z_j(t) = I_j(t) + iQ_j(t) = a_j(t) e^{i\theta_j(t)}, \tag{3}$$

where time functions $a_j(t)$ and $\theta_j(t)$ are called instantaneous amplitude and instantaneous phase functions, respectively, and $i^2 = -1$. The instantaneous frequency of the jth IMF is given by

$$\omega_j(t) = \frac{\mathrm{d}\theta_j(t)}{\mathrm{d}t}. \tag{4}$$

$a_j(t)$ and $\omega_j(t)$ $(j = 1, 2, \ldots, N)$ define the Hilbert amplitude spectrum, or simply Hilbert spectrum. Then, the original time series can be represented as follows:

$$X(t) = \mathrm{Re}\left\{\sum_{j=1}^{N} a_j(t) e^{i\theta_j(t)}\right\} + r(t). \tag{5}$$

Based on the above derivation, Wen and Gu [18] constructed the underlying random process model corresponding to an observational record by introducing a random element as follows:

$$X(t) = \mathrm{Re}\left\{\sum_{j=1}^{N} a_j(t) e^{i\left[\theta_j(t)+\varphi_j\right]}\right\} + r(t), \tag{6}$$

where φ_j's are independent random phase angles that are uniformly distributed between 0 and 2π. The mean and variance of the process are as follows:

$$\mu_x(t) = \mathrm{Re}\left\{\sum_{j=1}^{N} a_j(t) e^{i\theta_j(t)} E\left[e^{i\varphi_j}\right]\right\} + r(t) = r(t), \tag{7}$$

$$\sigma_x^2(t) = E\left\{\left[X(t) - \mu_x(t)\right]^2\right\} = \frac{1}{2}\sum_{j=1}^{N} a_j^2(t). \tag{8}$$

Then, the mean and variance of each component of $X(t)$ can be expressed as

$$\mu_{x,j}(t) = \mathrm{Re}\left\{a_j(t) e^{i\theta_j(t)} E\left[e^{i\varphi_j}\right]\right\} = 0, \quad j = 1, 2, \ldots, N, \tag{9}$$

$$\sigma_{x,j}^2(t) = E\left\{\left[X_j(t) - \mu_{x,j}(t)\right]^2\right\} = \frac{1}{2} a_j^2(t). \tag{10}$$

The Hilbert spectrum of each simulated sample is the same as that of the record; in other words, the ground motion simulated by using this method is ergodic in the sense of Hilbert spectrum. Thus, the ensemble average of the simulated Hilbert spectra is also identical with the target.

2.2. Random Amplitude-Based Improved Hilbert Spectral Representation Method. Based on the IMFs obtained from the underlying random process corresponding to a real earthquake record, SCEGMs possessing natural nonstationary characteristics can be simulated by means of a prescribed spatial correlation model [20]. The simulation procedure of the IHSRM is shown in Figure 1, where the N-S

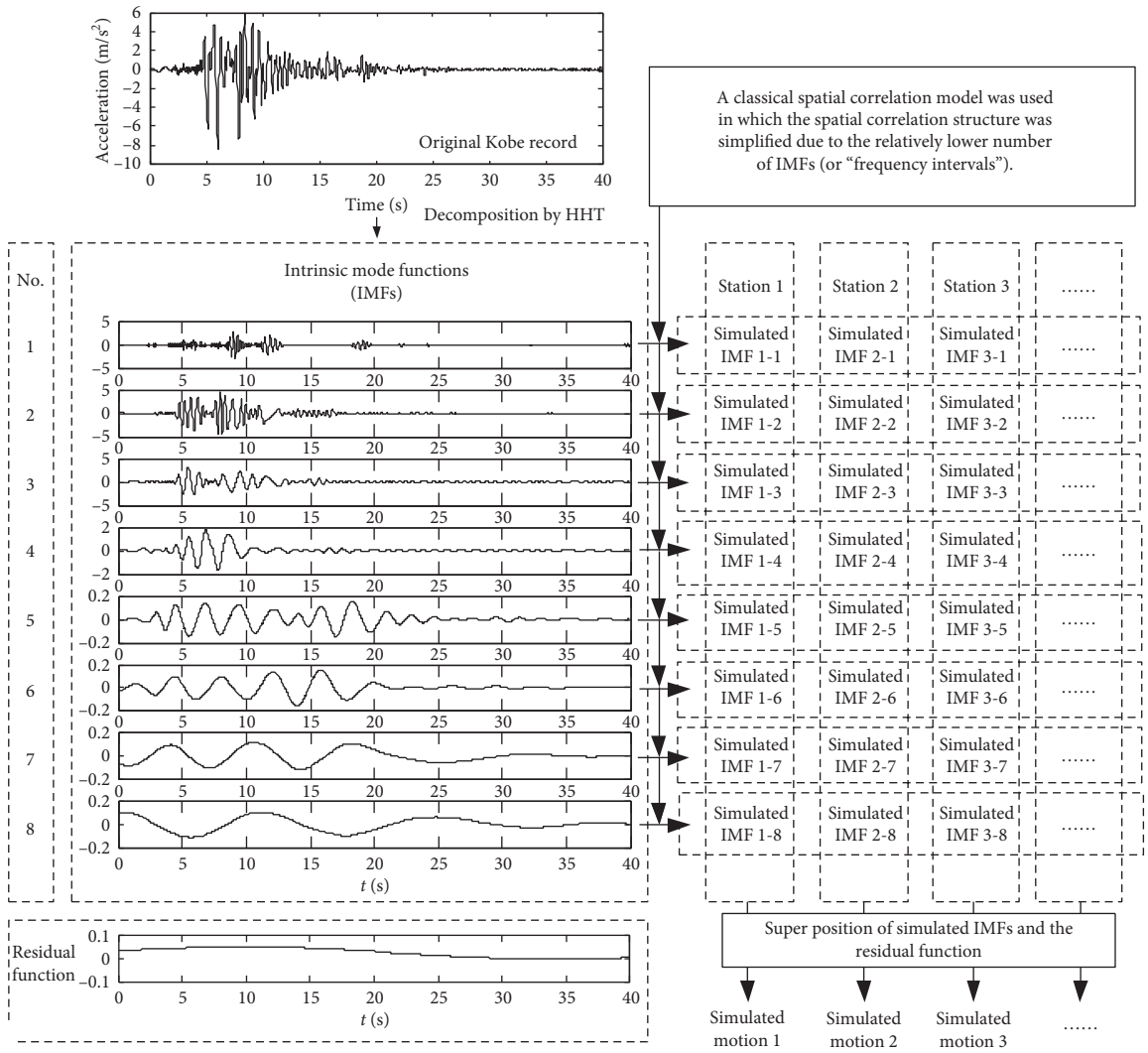

Figure 1: Simulation procedure of the IHSRM.

component of the 1995 Kobe earthquake is taken as an example.

Considering the correlation relations at the predominant frequency of each reference IMF and the Cholesky decomposition, the ground motion simulated by the random amplitude-based IHSRM at the mth station can be expressed as

$$x_m(t) = \sum_{k=1}^{m}\sum_{j=1}^{N}\sigma_j(t)D_{km,j}\left\{A_{kj}\cos\left[\theta_j(t)+\Phi_{km,j}\right]\right.$$
$$\left.+B_{kj}\sin\left[\theta_j(t)+\Phi_{km,j}\right]\right\}+r(t), \tag{11}$$
$$\Phi_{km,j} = -\frac{\omega_j\boldsymbol{\eta}_{km}}{V},$$

where $\sigma_j(t)$ is the ensemble variance of the jth IMF of the underlying random process, $D_{km,j}$ is an element of the decomposed spatial covariance matrix, $\boldsymbol{\eta}_{km}$ denotes the separation distance vector, and V is the apparent wave velocity in the medium; A_{kj} and B_{kj} denote independent and normally distributed zero-mean numbers with unit variance, obeying the following orthogonal relationships [21]:

$$E\left(A_{k1j1}A_{k2j2}\right) = \delta_{k1k2}\delta_{j1j2},$$
$$E\left(B_{k1j1}B_{k2j2}\right) = \delta_{k1k2}\delta_{j1j2}, \tag{12}$$
$$E\left(A_{k1j1}B_{k2j2}\right) = 0,$$

where δ_{kj} is the Kronecker delta function. The ensemble averages of mean and variance of seismic motions simulated by the random amplitude-based IHSRM had been proved to be equal to the targets which were derived using equations (7)–(10); the ensemble averaged Hilbert spectra of generated motions are also identical with the target (detailed derivation processes can be found in [20]). In the present procedure, the frequency dependence of the spatial correlation function is simplified so that only the correlation at the predominant frequency of each IMF is taken into consideration. Thus, the number of frequency intervals is extremely lower than that in the classical SRM. The double summation and matrix decomposition in the proposed formula are quite simplified.

In addition, the decomposition of a real correlation coefficient matrix is relatively faster. Therefore, the proposed method facilitates the generation of ground motions with higher efficiency.

3. Random Phase-Based Improved Hilbert Spectral Representation Method

The simulated and target IMFs of the same order are assumed to have the same standard variance σ and instantaneous frequency, which is a reasonable approach when the focus of an earthquake is located at a large distance from the site compared with the site dimension [22]. To facilitate the derivation, the predictable wave propagation effect is assumed to have been removed temporally and that the spatial correlation structures are known a priori [20]. The covariance matrix **COV** can be expressed in terms of variance σ^2 and the spatial correlation coefficient matrix **C** as given by

$$\mathbf{COV} = \sigma^2\mathbf{C} = \sigma^2\begin{bmatrix} 1 & C_{12} & \cdots & C_{1L} \\ C_{L1} & 1 & \cdots & C_{2L} \\ \vdots & \vdots & \ddots & \vdots \\ C_{L1} & C_{L2} & \cdots & 1 \end{bmatrix}_{(L\times L)}, \tag{13}$$

where C_{mn} (m, $n = 1, 2, \ldots, L$) is typically a real function of frequency and separation distance and L is the number of simulation stations.

To make the generated ground motions compatible with the individual function in **COV**, the ground motion at the mth station is assumed to be

$$x_m(t) = \mathrm{Re}\left\{\sum_{k=1}^{L}\sum_{j=1}^{N} A_{km,j}(t)e^{i\left[\theta_j(t)+\varphi_{k,j}\right]}\right\} + r(t), \quad m = 1, 2, \ldots, L, \tag{14}$$

where $A_{km,j}(t)$ denotes the instantaneous amplitude of the component IMF of the jth order by considering the correlations specified in equation (13). $A_{km,j}(t)$ can be determined by using the following algorithm.

The jth component IMF at the mth station can be expressed as

$$x_{m,j}(t) = \mathrm{Re}\left\{\sum_{k=1}^{L} A_{km,j}(t)e^{i\left[\theta_j(t)+\varphi_{k,j}\right]}\right\}, \quad j = 1, 2, \ldots, N. \tag{15}$$

Then, the cross-covariance between $x_{m,j}(t)$ and $x_{n,j}(t)$ is

$$\mathrm{Cov}\left[x_{m,j}(t), x_{n,j}(t)\right] = E\left\{\sum_{k=1}^{L}\mathrm{Re}\left\{A_{km,j}(t)e^{i\left[\theta_j(t)+\varphi_{k,j}\right]}\right\}\sum_{p=1}^{L}\mathrm{Re}\left\{A_{pn,j}(t)e^{i\left[\theta_j(t)+\varphi_{p,j}\right]}\right\}\right\}. \tag{16}$$

When $k \neq p$, the cross-covariance vanishes because $\varphi_{k,j}$ and $\varphi_{p,j}$ are statistically independent in such cases. Therefore,

$$\begin{aligned}\mathrm{Cov}\left[x_{m,j}(t), x_{n,j}(t)\right] &= E\left\{\sum_{k=1}^{L}\mathrm{Re}\left\{A_{km,j}(t)e^{i\left[\theta_j(t)+\varphi_{k,j}\right]}\right\}\mathrm{Re}\left\{A_{kn,j}(t)e^{i\left[\theta_j(t)+\varphi_{k,j}\right]}\right\}\right\} \\ &= \sum_{k=1}^{L}\frac{1}{2}A_{km,j}(t)A_{kn,j}(t)E\left[\cos\left(2\theta_j(t) + 2\varphi_{k,j}\right) + \cos(0)\right] \\ &= \sum_{k=1}^{L}\frac{1}{2}A_{km,j}(t)A_{kn,j}(t).\end{aligned} \tag{17}$$

In accordance with equations (10) and (13), the preceding cross-covariance at the jth order can also be expressed in terms of the spatial correlation coefficients in the following form:

$$\mathrm{Cov}\left[x_{m,j}(t), x_{n,j}(t)\right] = \sigma_j^2(t)C_{mn,j}, \tag{18}$$

where $\sigma_j^2(t)$ denotes the ensemble variance of the jth target IMF and $C_{mn,j}$ represents the spatial correlation coefficient between the mth and nth motions that corresponds to the predominant frequency of the jth target IMF, ω_j.

Matrix $\mathbf{C}_j$ is usually symmetric and positive defined; therefore, it can usually be decomposed into the multiplication of two identical and symmetric matrices by utilizing the root decomposition process proposed by Wu et al. [23–25], which is described as follows:

$$\sigma_j^2(t)\mathbf{C}_j = \sigma_j^2(t)\mathbf{D}_j\mathbf{D}_j^T, \tag{19}$$

$$\sigma_j^2(t)C_{mn,j} = \sigma_j^2(t)\sum_{k=1}^{L} D_{km,j}D_{kn,j}, \tag{20}$$

where T indicates the transpose of a matrix.

Then, the following formula can be obtained:

$$\sum_{k=1}^{L}\frac{1}{2}A_{km,j}(t)A_{kn,j}(t) = \sigma_j^2(t)C_{mn,j} = \sigma_j^2(t)\sum_{k=1}^{L} D_{km,j}D_{kn,j}. \tag{21}$$

Comparing the corresponding terms on both sides of equation (21) yields

$$A_{km,j}(t) = \sqrt{2\sigma_j^2(t)}D_{km,j} = a_j(t)D_{km,j}. \tag{22}$$

Then, the SCEGMs that consider the wave propagation effect can be obtained as follows:

$$x_m(t) = \sum_{k=1}^{L}\sum_{j=1}^{N}\sqrt{2\sigma_j^2(t)}D_{km,j}\cos\left[\theta_j(t) + \Phi_{km,j} + \varphi_{k,j}\right] + r(t), \tag{23}$$

$$\Phi_{km,j} = -\frac{\omega_j\left|\boldsymbol{\eta}_{km}\right|}{V}. \tag{24}$$

To summarize the procedure as presented, the simulation of SCEGMs consists of the following steps: (i) $A_{km,j}(t)$ is computed using equations (13)–(22) based on a spatial correlation model for "phase-aligned" ground motions; (ii) the SCEGM for each simulation station is obtained using equations (23) and (24) by considering the wave propagation effect and the summation of simulated IMFs and the original residual function.

To construct the spatial covariance matrix shown in equation (13), the isotropic frequency-dependent correlation coefficient model used by Vanmarcke et al. [26, 27] and Zerva and Shinozuka [28] to simulate "phase-aligned" earthquake ground motions can be adopted:

$$C(\boldsymbol{\eta}_{mn}) = \exp\left[-\frac{\omega\left|\boldsymbol{\eta}_{mn}\right|}{2\pi V d}\right], \tag{25}$$

where d is the correlation distance, and $d > 0$. A large d value is expected to demonstrate high correlation between points of the random field. The covariance function for the jth components can be expressed as

$$\mathrm{COV}_{mn,j} = \sigma_j^2(t)C_j(\boldsymbol{\eta}_{mn}) = \sigma_j^2(t)\exp\left[-\frac{\omega_j\left|\boldsymbol{\eta}_{mn}\right|}{2\pi V d}\right]. \tag{26}$$

The ensemble averages of the mean and variance of $x_m(t)$ and $x_{m,j}(t)$ are determined to be identical with those of the target underlying random process and the jth reference IMF, respectively (see Appendix A). The Hilbert spectra of the sample realizations of this model differ, but $C_{mm,j} = 1$ ensures that the ensemble average of the Hilbert spectra of the samples is the same as the target Hilbert spectrum, which is also proven in Appendix A. Note that since only the predominant frequencies of reference IMFs were considered, the IHSRM-simulated random processes are not periodic.

Taking the E-W component of the 2011 Niigata earthquake in Japan as the reference, a group of SCEGMs are simulated for three locations to demonstrate the reliability of the present method, in which $d = 100$, and the spacing distance is set to 100 m. The original record and the corresponding generated ground motions are shown in Figure 2. It can be found that the waveform of the simulated motions is significantly close to the target motion. The acceleration response spectra of the original record and simulated motions are compared in Figure 3, and good match can be observed. In addition, the ensemble average correlation coefficients between simulated ground motions derived from 2,000 simulations are compared with the corresponding target values as shown in Figure 4. The simulation values of correlation coefficients are approximately identical with the targets, which verifies the validness of the proposed method.

4. Error Assessment

The decomposition of the spatial correlation coefficient matrix involved in the IHSRM can usually be carried out by Cholesky decomposition, root decomposition, or eigendecomposition. Thus, different combinations of the simulation formulas with the decomposition methods yield a distinction between these six types of IHSRMs: random phase formula and Cholesky decomposition-based IHSRM (RP-CIHSRM); random phase formula and root decomposition-based IHSRM (RP-RIHSRM); random phase formula and eigendecomposition-based IHSRM (RP-EIHSRM); random amplitude formula and Cholesky decomposition-based IHSRM (RA-CIHSRM); random amplitude formula and root decomposition-based IHSRM (RA-RIHSRM); and random amplitude formula and eigendecomposition-based IHSRM (RA-EIHSRM). Despite the difference among the three different decomposition methods, the formulas for these IHSRMs can be unified as follows.

For RP-IHSRM,

$$x_m(t) = \sum_{k=1}^{L}\sum_{j=1}^{N} a_j(t)D_{km,j}\cos\left[\theta_j(t) + \Phi_{km,j} + \varphi_{k,j}\right] + r(t). \tag{27}$$

For RA-IHSRM,

$$\begin{aligned} x_m(t) = \sum_{k=1}^{L}\sum_{j=1}^{N}\sigma_j(t)D_{km,j}\Big\{&A_{kj}\cos\left[\theta_j(t) + \Phi_{km,j}\right] \\ &+ B_{kj}\sin\left[\theta_j(t) + \Phi_{km,j}\right]\Big\} + r(t). \end{aligned} \tag{28}$$

When different decomposition methods are employed, only $D_{km,j}$'s are different.

In this section, the N-S component of the 1995 Kobe earthquake in Japan was selected as the reference motion, and SCEGMs will be generated for three locations spaced at 100 m intervals (0, 100, and 200 m) along the direction of

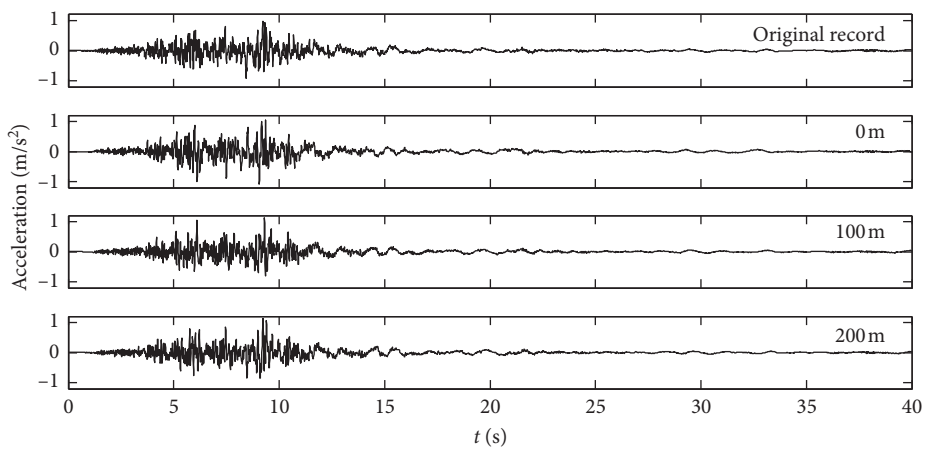

Figure 2: Comparison of acceleration-time histories of simulated ground motions with the original record.

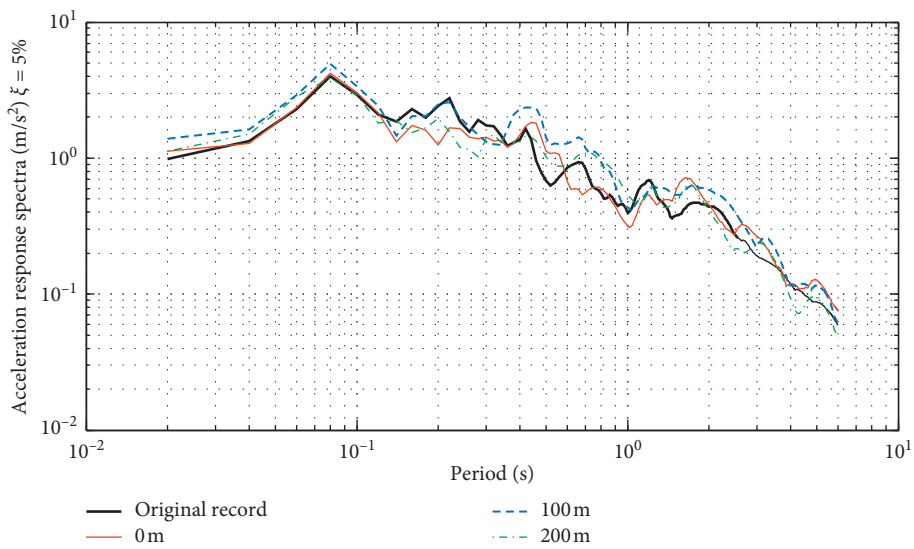

Figure 3: The acceleration response spectra of simulated ground motions and the original record.

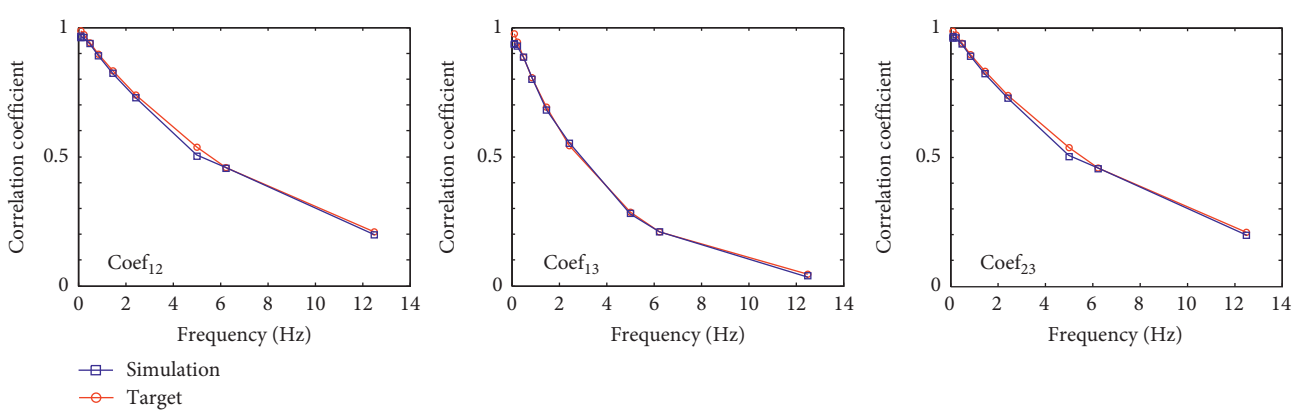

(a)

Figure 4: Continued.

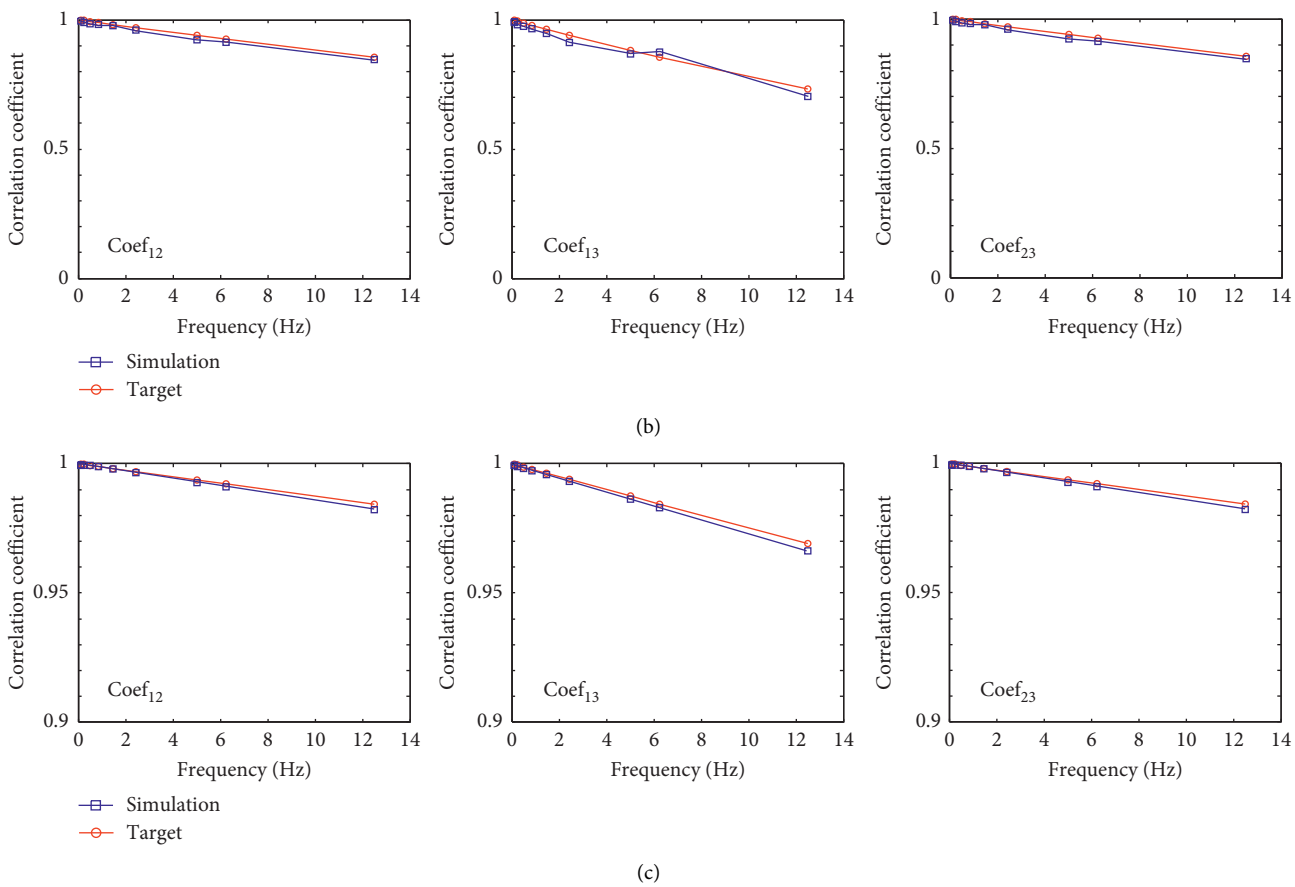

Figure 4: Comparison of the ensemble average correlation coefficients between simulated ground motions with targets: (a) $d = 1$; (b) $d = 10$; (c) $d = 100$.

wave propagation to proceed with the error assessment. Then, based on the unified simulation formulas, an error analysis of random processes simulated by the aforementioned IHSRMs is conducted, and the results are compared to facilitate the selection of the optimal type of IHSRM.

4.1. Definition of Errors. The bias error $b(\cdot)$ and the stochastic error $\sigma(\cdot)$ [29] were adopted to proceed with the error assessment which are shown as follows:

$$b\left(\vartheta^T\right) = E\left(\vartheta^T\right) - \vartheta^0, \tag{29}$$

$$\sigma\left(\vartheta^T\right) = \sqrt{E\left(\vartheta^T\right)^2 - E^2\left(\vartheta^T\right)} = \sqrt{E\left[\vartheta^T - E\left(\vartheta^T\right)\right]^2}, \tag{30}$$

where ϑ denotes one type of the temporal statistic of the simulated process and superscript T represents that the temporal statistic is obtained by estimating over the entire time duration; superscript 0 is the target value. The bias error can measure the degree that the ensemble average of the temporal estimation deviates from the corresponding target. By contrast, the stochastic error can measure the degree that the temporal estimation fluctuates around its ensemble average.

4.2. Bias Error and Stochastic Error of the Mean. Note that the ensemble average of mean, variance, and Hilbert spectra of seismic motions simulated by the RA-IHSRM had been proved to be equal to the target [20]. Appendix A has proved that the ensemble average of mean of $x_m(t)$ for the random phase method equates to the target. Therefore, the bias errors of mean of the component $x_m(t)$ are zero for these six types of formulas. For the random phase formulas, the stochastic error of mean of $x_m(t)$ can be expressed as

$$\begin{aligned}\sigma[\mu_m(t)] &= \sqrt{E[\mu_m(t)]^2 - E^2[\mu_m(t)]} \\ &= \sqrt{E\left\{\left\{\sum_{k1=1}^{L}\sum_{j1=1}^{N} a_{j1}(t)D_{k1m,j1}\cos\left[\theta_{j1}(t)+\varphi_{k1,j1}\right]+r(t)\right\}\cdot\left\{\sum_{k2=1}^{L}\sum_{j2=1}^{N} a_{j2}(t)D_{k2m,j2}\cos\left[\theta_{j2}(t)+\varphi_{k2,j2}\right]+r(t)\right\}\right\}-[r(t)]^2} \\ &= \sqrt{\sum_{k=1}^{L}\sum_{j=1}^{N}\frac{1}{2}a_j^2(t)D_{km,j}^2} \\ &= \sqrt{\sum_{j=1}^{N}\frac{1}{2}a_j^2(t)}.\end{aligned} \tag{31}$$

For the random amplitude formulas, the stochastic error of mean of $x_m(t)$ can be expressed as

$$\begin{aligned}\sigma[\mu_m(t)] &= \sqrt{E[\mu_m(t)]^2 - E^2[\mu_m(t)]} \\ &= \sqrt{E\left\{\left\{\sum_{k1=1}^{L}\sum_{j1=1}^{N} \sigma_{j1}(t)D_{k1m,j1}\left\{A_{k1j1}\cos\left[\theta_{j1}(t)\right]+B_{k1j1}\sin\left[\theta_{j1}(t)\right]\right\}+r(t)\right\}\cdot\left\{\sum_{k2=1}^{L}\sum_{j2=1}^{N} \sigma_{j2}(t)D_{k2m,j2}\left\{A_{k2j2}\cos\left[\theta_{j2}(t)\right]+B_{k2j2}\sin\left[\theta_{j2}(t)\right]\right\}+r(t)\right\}\right\}-[r(t)]^2} \\ &= \sqrt{\sum_{k=1}^{L}\sum_{j=1}^{N}\frac{1}{2}a_j^2(t)D_{km,j}^2} \\ &= \sqrt{\sum_{j=1}^{N}\frac{1}{2}a_j^2(t)}.\end{aligned} \tag{32}$$

From the stochastic errors presented above, it can be concluded that the IHSRM is not ergodic in terms of temporal mean.

4.3. Bias Error and Stochastic Error of the Variance. According to Appendix A and [20], the bias errors of variance of the component $x_m(t)$ simulated by random phase- and random amplitude-based IHSRMs are also zero.

For random phase formulas, the raw estimate of variance of $x_m(t)$ is

$$\widehat{\sigma}_m^2(t) = \left\{\sum_{k1=1}^{L}\sum_{j1=1}^{N} a_{j1}(t)D_{k1m,j1}\cos\left[\theta_{j1}(t)+\varphi_{k1,j1}\right]\right\}\cdot\left\{\sum_{k2=1}^{L}\sum_{j2=1}^{N} a_{j2}(t)D_{k2m,j2}\cos\left[\theta_{k2}(t)+\varphi_{k2,j2}\right]\right\}. \tag{33}$$

Then, for random phase formulas, the stochastic error of variance of $x_m(t)$ can be derived as follows:

$$\sigma\left[\widetilde{\sigma}_m^2(t)\right] = \left\{E\left\{\left\{\sum_{k1=1}^{L}\sum_{j1=1}^{N} a_{j1}(t)D_{k1m,j1}\cos\left[\theta_{j1}(t)+\varphi_{k1,j1}\right]\right\}\cdot\left\{\sum_{k2=1}^{L}\sum_{j2=1}^{N} a_{j2}(t)D_{k2m,j2}\cos\left[\theta_{j2}(t)+\varphi_{k2,j2}\right]\right\}\right\}^2 - \left[\sum_{j=1}^{N}\frac{1}{2}a_j^2(t)\right]^2\right\}^{1/2}$$
$$= \left\{\sum_{k=1}^{L}\sum_{j=1}^{N}\frac{3}{8}a_j^4(t)D_{km,j}^4 + \sum_{k=1}^{L}\sum_{\substack{p=1\\p\neq k}}^{L}\sum_{j=1}^{N}\sum_{\substack{q=1\\q\neq j}}^{N}\frac{3}{4}a_j^2(t)a_q^2(t)D_{km,j}^2D_{pm,q}^2 - \left[\sum_{j=1}^{N}\frac{1}{2}a_j^2(t)\right]^2\right\}^{1/2}. \tag{34}$$

For random amplitude formulas, the stochastic error of variance of $x_m(t)$ can be derived as follows:

$$\sigma\left[\widetilde{\sigma}_m^2(t)\right] = \left\{E\left\{\left\{\sum_{k1=1}^{L}\sum_{j1=1}^{N}\sigma_{j1}(t)D_{k1m,j1}\left\{A_{k1j1}\cos\left[\theta_{j1}(t)\right]+B_{k1j1}\sin\left[\theta_{j1}(t)\right]\right\}+r(t)\right\}\cdot\left\{\sum_{k2=1}^{L}\sum_{j2=1}^{N}\sigma_{j2}(t)D_{k2m,j2}\left\{A_{k2j2}\cos\left[\theta_{j2}(t)\right]+B_{k2j2}\sin\left[\theta_{j2}(t)\right]\right\}+r(t)\right\}\right\}^2 - \left[\sum_{j=1}^{N}\frac{1}{2}a_j^2(t)\right]^2\right\}^{1/2}$$
$$= \left\{\sum_{k=1}^{L}\sum_{j=1}^{N}\frac{3}{4}a_j^4(t)D_{km,j}^4 + \sum_{k=1}^{L}\sum_{\substack{p=1\\p\neq k}}^{L}\sum_{j=1}^{N}\sum_{\substack{q=1\\q\neq j}}^{N}\frac{3}{4}a_j^2(t)a_q^2(t)D_{km,j}^2D_{pm,q}^2 - \left[\sum_{j=1}^{N}\frac{1}{2}a_j^2(t)\right]^2\right\}^{1/2}. \tag{35}$$

The specific derivation process is shown in Appendix B.

4.4. Bias Error and Stochastic Error of the Cross-Covariance. Taking equations (8) and (10) and the property of cross-covariance into account, the target cross-covariance between $x_m(t)$ and $x_n(t)$ can be expressed as

$$\mathrm{COV}_{mn}^0(t) = \sum_{j=1}^{N}\mathrm{COV}_{mn,j}^0(t) = \sum_{j=1}^{N}\frac{1}{2}a_j^2(t)C_{mn,j}. \tag{36}$$

For random phase- and random amplitude-based IHSRMs, the raw estimates of cross-covariance between $x_m(t)$ and $x_n(t)$ (m, $n = 1, 2, 3$) are

$$\widehat{\mathrm{COV}}_{mn}(t) = \left\{\sum_{k1=1}^{L}\sum_{j1=1}^{N} a_{j1}(t)D_{k1m,j1}\cos\left[\theta_{j1}(t)+\varphi_{k1,j1}\right]\right\}\cdot\left\{\sum_{k2=1}^{L}\sum_{j2=1}^{N} a_{j2}(t)D_{k2n,j2}\cos\left[\theta_{j2}(t)+\varphi_{k2,j2}\right]\right\},$$
$$\widehat{\mathrm{COV}}_{mn}(t) = \left\{\sum_{k1=1}^{L}\sum_{j1=1}^{N}\sigma_{j1}(t)D_{k1m,j1}\left\{A_{k1j1}\cos\left[\theta_{j1}(t)\right]+B_{k1j1}\sin\left[\theta_{j1}(t)\right]\right\}\right\}\cdot\left\{\sum_{k2=1}^{L}\sum_{j2=1}^{N}\sigma_{j2}(t)D_{k2n,j2}\left\{A_{k2j2}\cos\left[\theta_{j2}(t)\right]\right.\right.$$
$$\left.\left.+B_{k2j2}\sin\left[\theta_{j2}(t)\right]\right\}\right\}. \tag{37}$$

Performing mathematical expectation on $\widehat{\mathrm{COV}}_{mn}(t)$'s yields

$$E\left[\widehat{\mathrm{COV}}_{mn}(t)\right] = E\left\{\left\{\sum_{k=1}^{L}\sum_{j=1}^{N}\sqrt{2\sigma_j^2(t)}\,D_{km,j}\cos\left[\theta_j(t)+\varphi_{k,j}\right]\right\}\cdot\left\{\sum_{p=1}^{L}\sum_{q=1}^{N}\sqrt{2\sigma_q^2(t)}\,D_{pn,q}\cos\left[\theta_q(t)+\varphi_{p,q}\right]\right\}\right\}$$
$$= \sum_{j=1}^{N}\frac{1}{2}a_j^2(t)C_{mn,j}, \tag{38}$$

$$E\left[\widehat{\mathrm{COV}}_{mn}(t)\right] = E\left\{\left\{\sum_{k1=1}^{L}\sum_{j1=1}^{N}\sigma_{j1}(t)D_{k1m,j1}\left\{A_{k1j1}\cos\left[\theta_{j1}(t)\right]+B_{k1j1}\sin\left[\theta_{j1}(t)\right]\right\}\right\}\cdot\left\{\sum_{k2=1}^{L}\sum_{j2=1}^{N}\sigma_{j2}(t)D_{k2m,j2}\left\{A_{k2j2}\cos\left[\theta_{j2}(t)\right]\right.\right.$$
$$\left.\left.+B_{k2j2}\sin\left[\theta_{j2}(t)\right]\right\}\right\}\right\}$$
$$= \sum_{j=1}^{N}\frac{1}{2}a_j^2C_{mn,j}. \tag{39}$$

Thus, the bias errors of cross-covariance for both random phase- and random amplitude-based IHSRMs can be expressed as

$$b\left[\widehat{\mathrm{COV}}_{mn}(t)\right] = E\left[\widehat{\mathrm{COV}}_{mn}(t)\right] - \mathrm{COV}_{mn}^{0}(t) = 0. \tag{40}$$

The stochastic errors of cross-covariance for random phase and random amplitude formulas can be derived as follows (see Appendix C for a detailed proof):

$$\sigma\left[\widehat{\mathrm{COV}}_{mn}(t)\right] = \left\{E\left\{\left\{\sum_{k1=1}^{L}\sum_{j1=1}^{N}a_{j1}(t)D_{k1m,j1}\cos\left[\theta_{j1}(t)+\varphi_{k1,j1}\right]\right\}\cdot\left\{\sum_{k2=1}^{L}\sum_{j2=1}^{N}a_{j2}(t)D_{k2n,j2}\cos\left[\theta_{j2}(t)+\varphi_{k2,j2}\right]\right\}\right\}^2-\left[\sum_{j=1}^{N}\frac{1}{2}a_j^2(t)C_{mn,j}\right]^2\right\}^{1/2}$$
$$= \left\{\sum_{k=1}^{L}\sum_{j=1}^{N}\frac{3}{8}a_j^4(t)D_{km,j}^2D_{kn,j}^2+2\sum_{k=1}^{L}\sum_{\substack{p=1\\p\neq k}}^{L}\sum_{j=1}^{N}\sum_{\substack{q=1\\q\neq j}}^{N}\frac{1}{4}a_j^2(t)a_q^2(t)D_{km,j}D_{kn,j}D_{pm,q}D_{pn,q}+\sum_{k=1}^{L}\sum_{\substack{p=1\\p\neq k}}^{L}\sum_{j=1}^{N}\sum_{\substack{q=1\\q\neq j}}^{N}\frac{1}{4}a_j^2(t)a_q^2(t)D_{km,j}^2D_{pn,q}^2-\left[\sum_{j=1}^{N}\frac{1}{2}a_j^2(t)C_{mn,j}\right]^2\right\}^{1/2}, \tag{41}$$

$$\sigma\left[\widehat{COV}_{mn}(t)\right] = \left\{E\left\{\left\{\sum_{k1=1}^{L}\sum_{j1=1}^{N}\sigma_{j1}(t)D_{k1m,j1}\left\{A_{k1j1}\cos\left[\theta_{j1}(t)\right]+B_{k1j1}\sin\left[\theta_{j1}(t)\right]\right\}+r(t)\right\}\right.\right.$$
$$\left.\left.\cdot\left\{\sum_{k2=1}^{L}\sum_{j2=1}^{N}\sigma_{j2}(t)D_{k2n,j2}\left\{A_{k2j2}\cos\left[\theta_{j2}(t)\right]+B_{k2j2}\sin\left[\theta_{j2}(t)\right]\right\}+r(t)\right\}\right\}^2-\left[\sum_{j=1}^{N}\frac{1}{2}a_j^2(t)C_{mn,j}\right]^2\right\}^{1/2}$$
$$= \left\{\sum_{k=1}^{L}\sum_{j=1}^{N}\frac{3}{4}a_j^4(t)D_{km,j}^2D_{kn,j}^2+2\sum_{k=1}^{L}\sum_{\substack{p=1\\p\neq k}}^{L}\sum_{j=1}^{N}\sum_{\substack{q=1\\q\neq j}}^{N}\frac{1}{4}a_j^2(t)a_q^2(t)D_{km,j}D_{kn,j}D_{pm,q}D_{pn,q}\right.$$
$$\left.+\sum_{k=1}^{L}\sum_{\substack{p=1\\p\neq k}}^{L}\sum_{j=1}^{N}\sum_{\substack{q=1\\q\neq j}}^{N}\frac{1}{4}a_j^2(t)a_q^2(t)D_{km,j}^2D_{pn,q}^2-\left[\sum_{j=1}^{N}\frac{1}{2}a_j^2(t)C_{mn,j}\right]^2\right\}^{1/2} \tag{42}$$

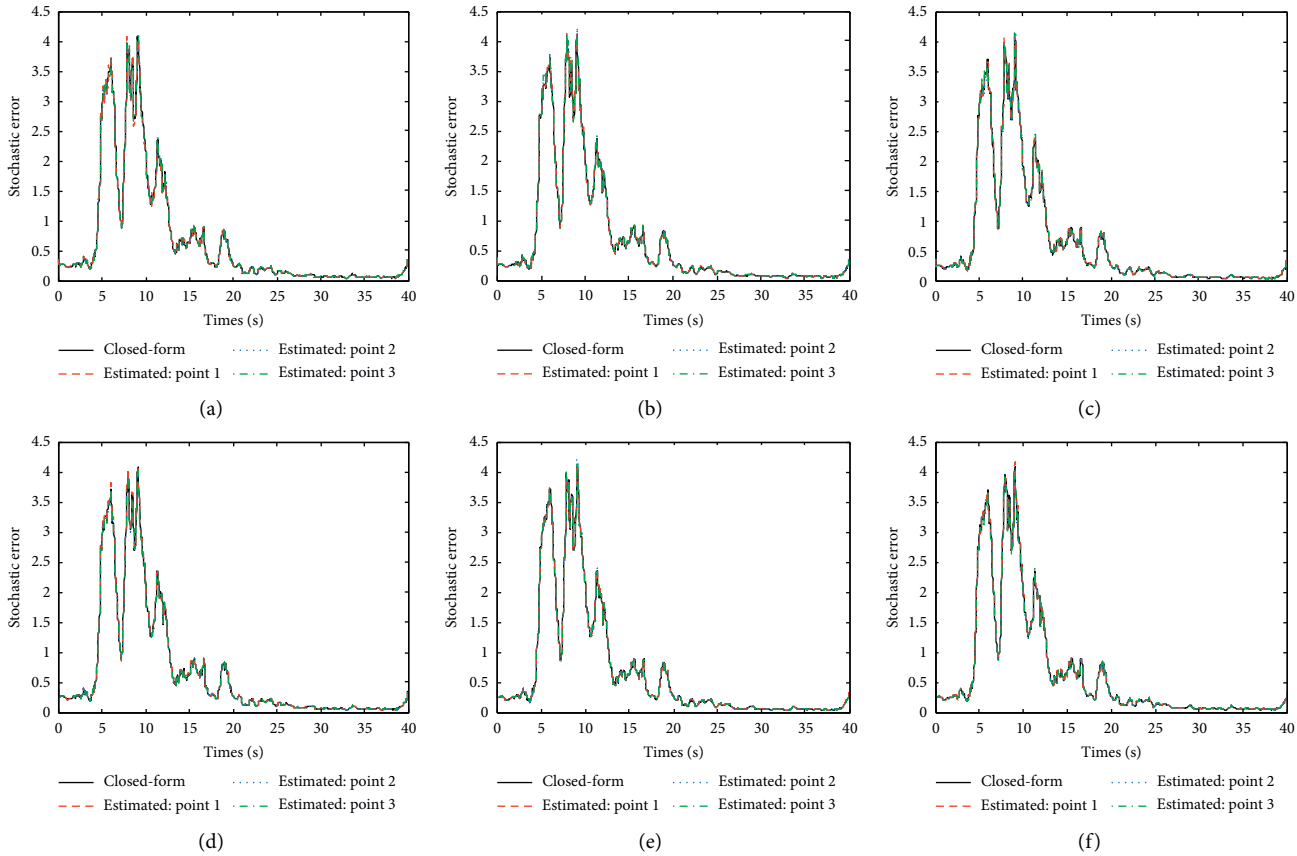

Figure 5: Comparison between the closed-form and estimated stochastic errors of temporal mean among the six types of methods: (a) RP-CIHSRM; (b) RP-RIHSRM; and (c) RP-EIHSRM; (d) RA-CIHSRM; (e) RA-RIHSRM; and (f) RA-EIHSRM.

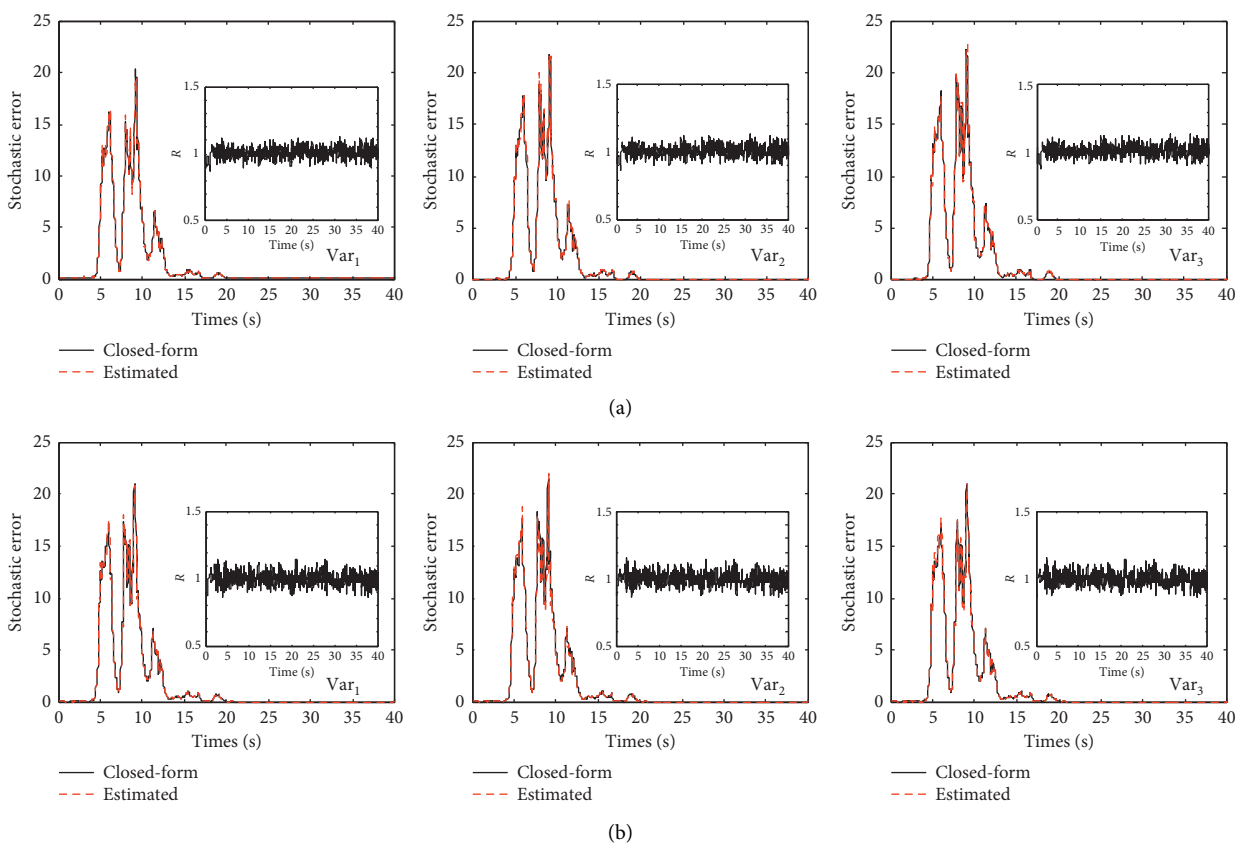

Figure 6: Continued.

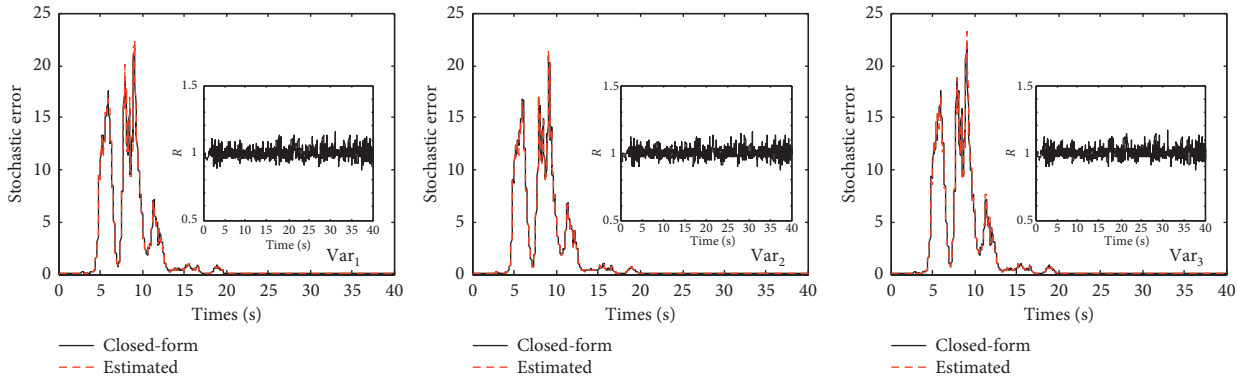

(c)

Figure 6: Comparison between the closed-form and estimated stochastic errors of temporal variance: (a) RP-CIHSRM; (b) RP-RIHSRM; (c) RP-EIHSRM.

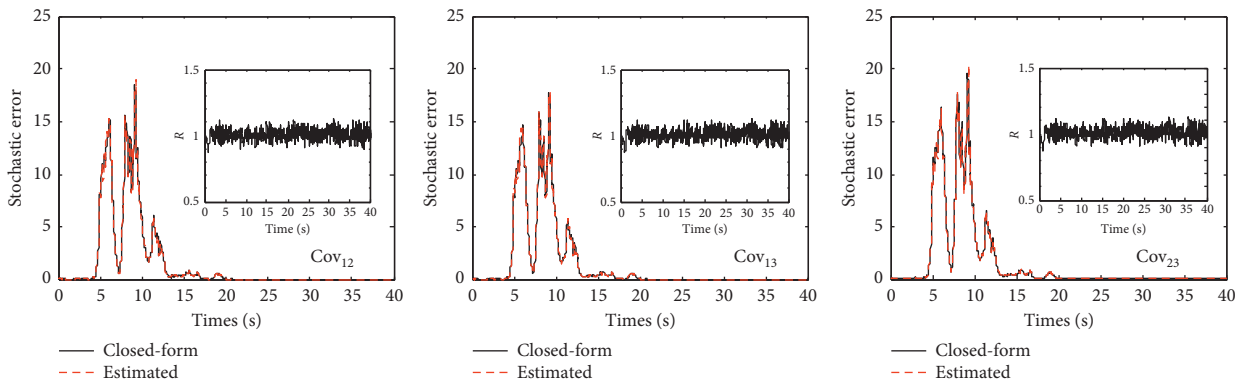

(a)

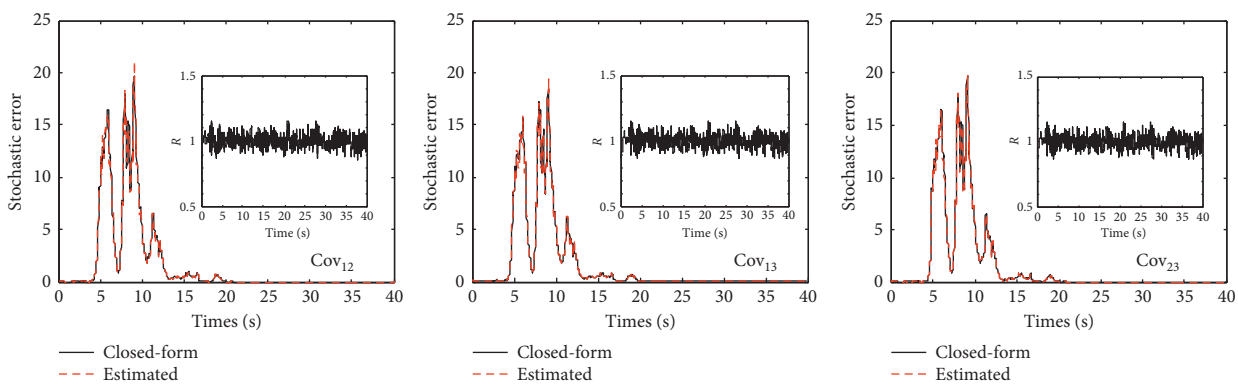

(b)

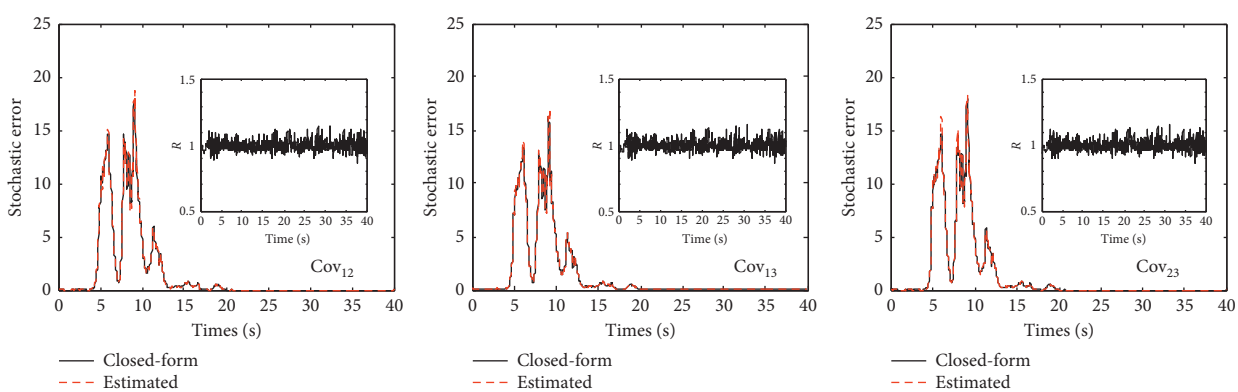

(c)

Figure 7: Comparison between the closed-form and estimated stochastic errors of temporal cross-covariance: (a) RP-CIHSRM; (b) RP-RIHSRM; (c) RP-EIHSRM.

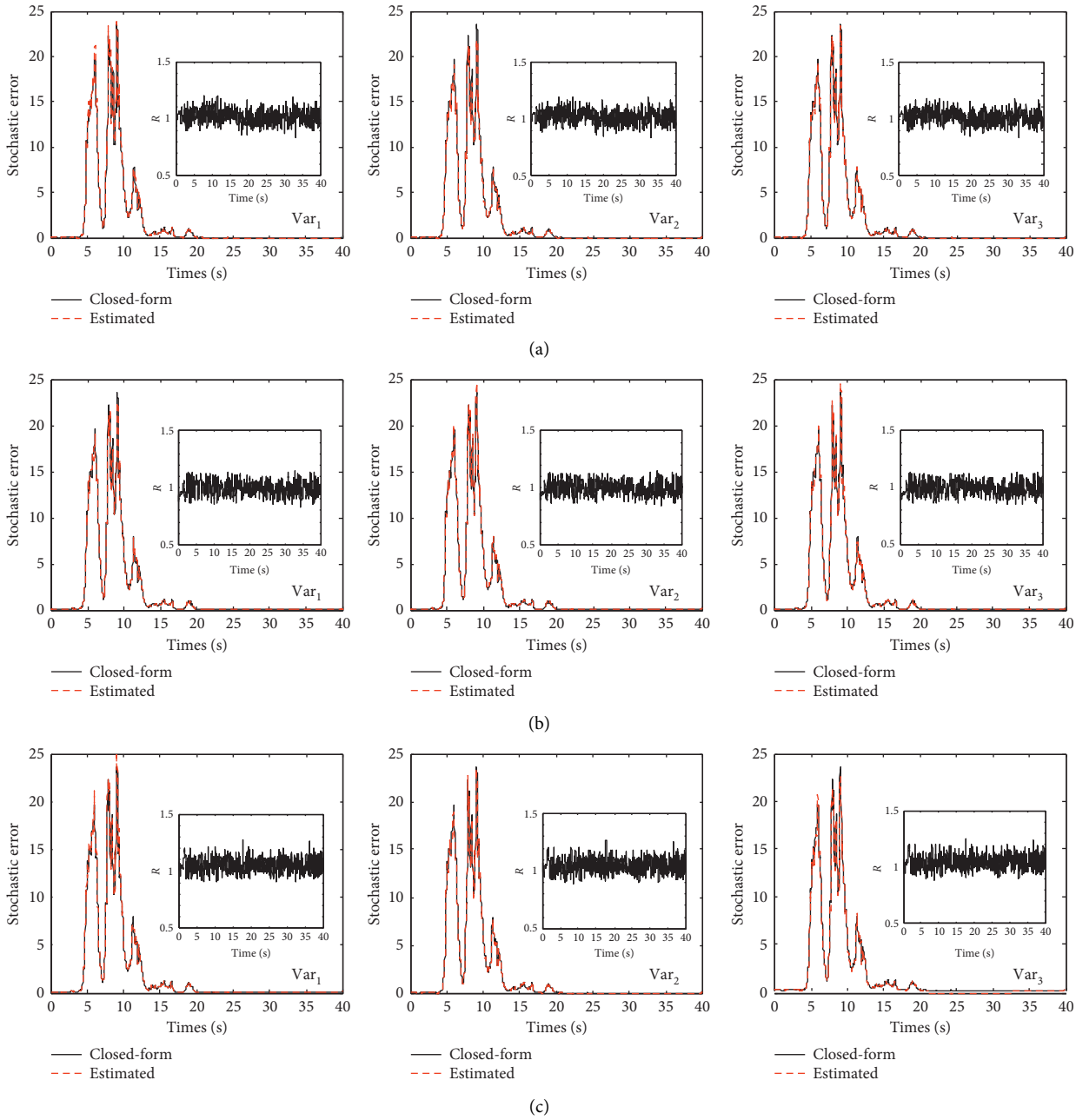

Figure 8: Comparison between the closed-form and estimated stochastic errors of temporal variance: (a) RA-CIHSRM; (b) RA-RIHSRM; (c) RA-EIHSRM.

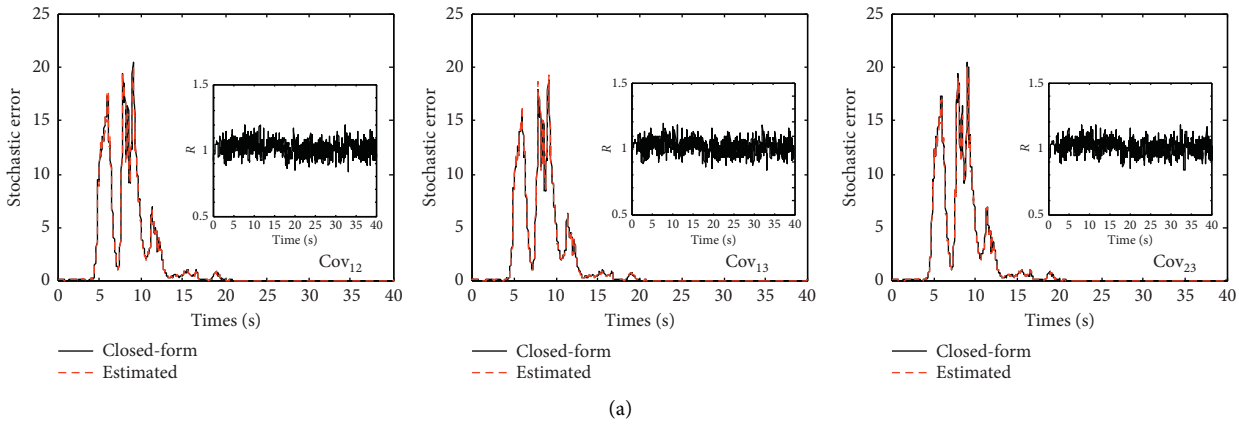

Figure 9: Continued.

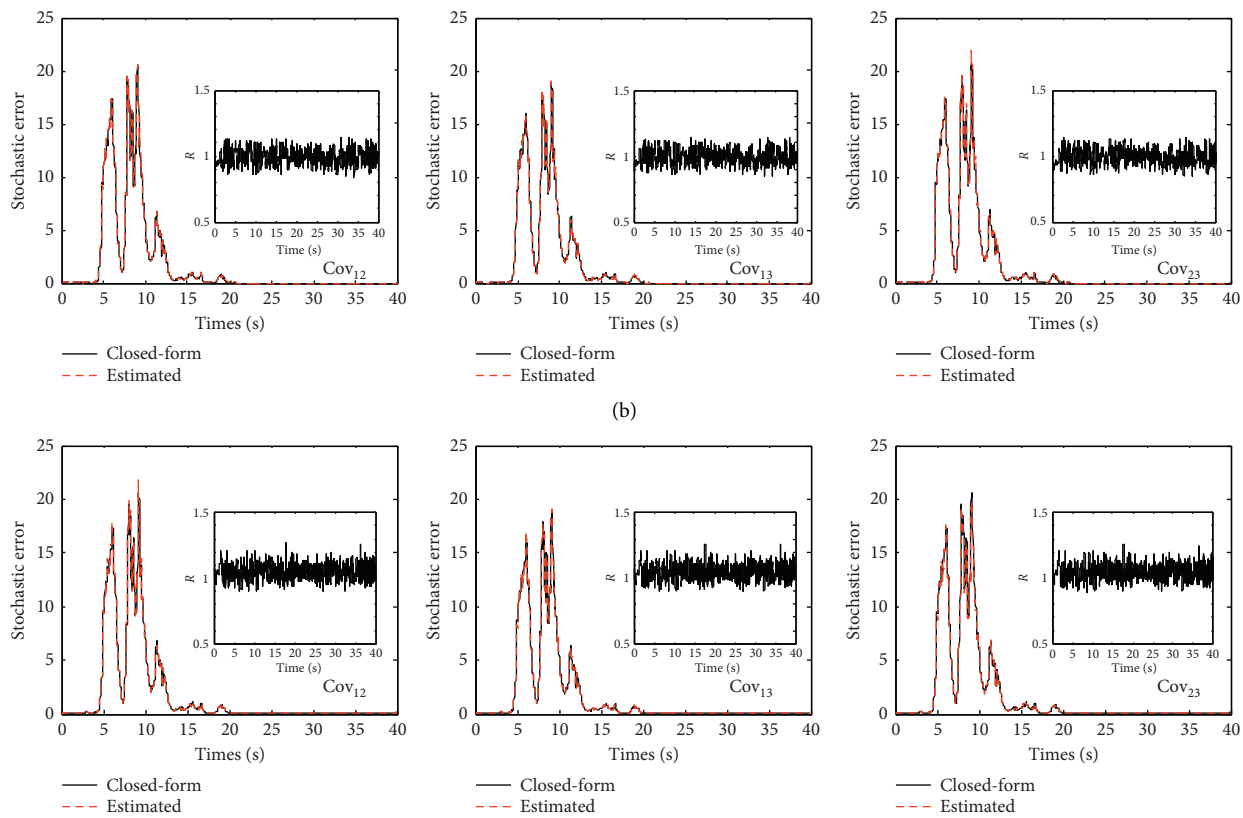

Figure 9: Comparison between the closed-form and estimated stochastic errors of temporal cross-covariance: (a) RA-CIHSRM; (b) RA-RIHSRM; (c) RA-EIHSRM.

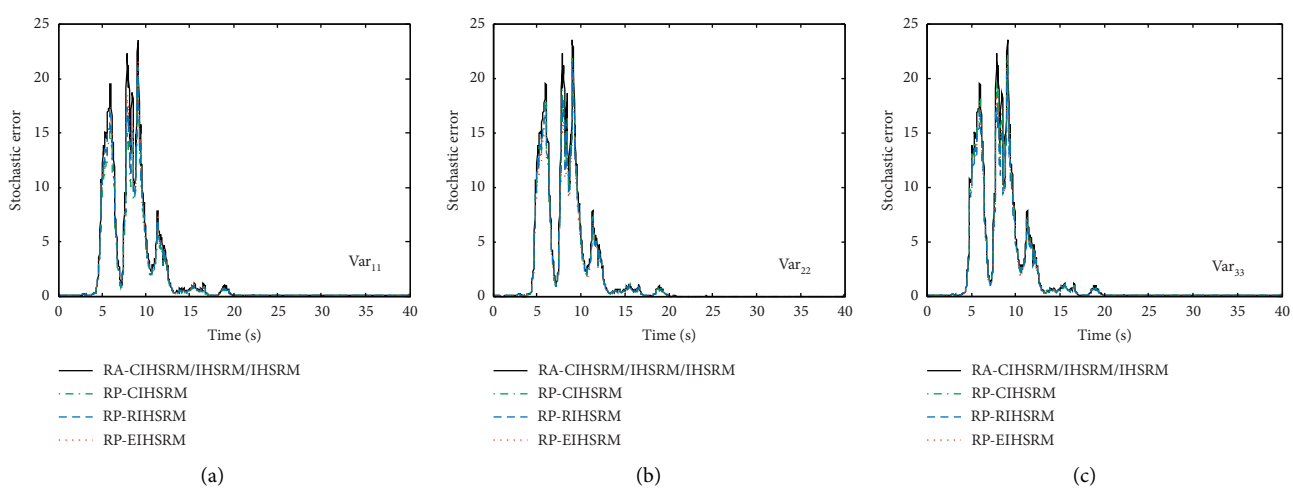

Figure 10: Continued.

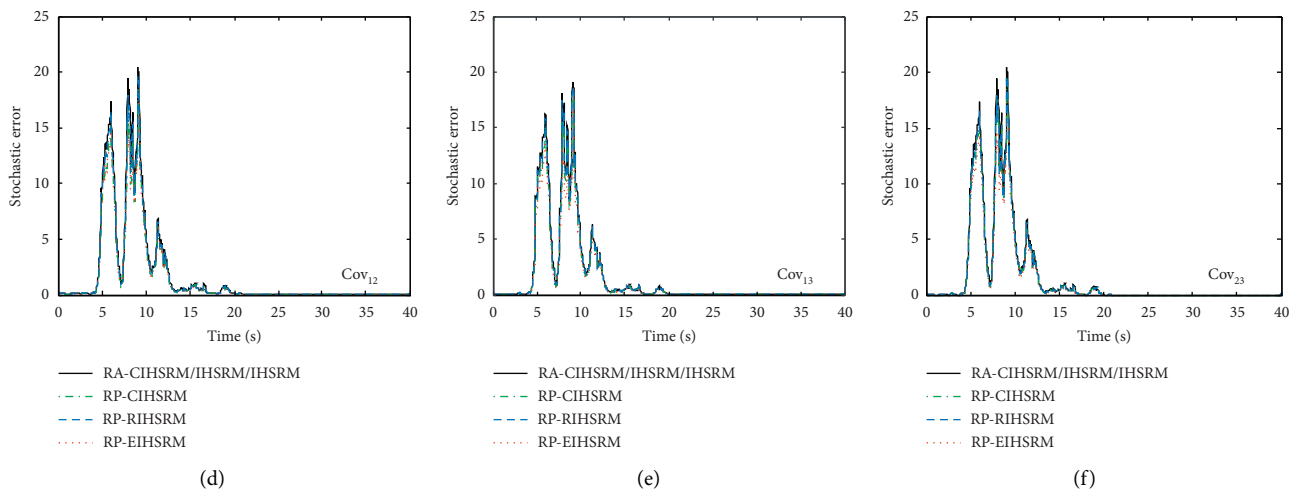

Figure 10: Comparison of the closed-form stochastic errors of temporal covariance among the six types of methods: (a) Var11; (b) Var22; and (c) Var33; (d) Cov12; (e) Cov13; and (f) Cov23.

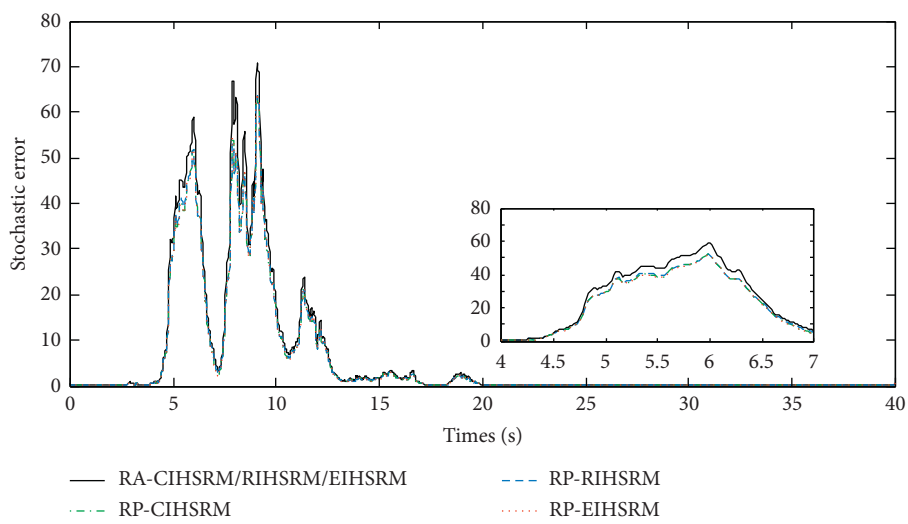

Figure 11: Sum of the stochastic errors of variance for different methods.

4.5. Verification and Discussion. To verify the closed-form stochastic errors of the temporal mean, variance, and cross-covariance, 2,000 sample processes were simulated for each of these six types of IHSRMs aforementioned. The estimated stochastic errors of mean for the six types of IHSRMs are compared with the corresponding closed-form ones in Figure 5. The estimated stochastic errors of variance and cross-covariance in comparison with the corresponding closed-form ones for RP-IHSRMs are shown in Figures 6 and 7, respectively. For RA-IHSRMs, the comparison between the estimated and closed-form stochastic errors of variance and cross-covariance is shown in Figures 8 and 9, respectively. In Figures 6–9, R denotes the ratio between closed-form and estimated stochastic errors. It can be found that the estimated temporal errors for each decomposition method match the corresponding closed-form ones very well, which verifies the validness of the derived closed-form solutions. Simultaneously, for all the six types of IHSRMs, the closed-form and estimated stochastic errors of cross-covariance between points 1 and 3 are slightly lower than those between points 1 and 2 and those between points 2 and 3 due to the loss of spatial correlation.

Figure 10 shows the comparison of the closed-form stochastic errors of temporal covariance (including variance and cross-covariance) among the six types of methods. For the three RA-IHSRMs, the closed-form stochastic errors of temporal covariance are identical, which demonstrates that the stochastic error of temporal covariance produced by RA-IHSRMs is independent of the matrix decomposition method. By contrast, the closed-form stochastic errors of temporal covariance produced by RP-IHSRMs are slightly different from each other. In addition, the stochastic errors of RA-IHSRMs are mildly higher than those of RP-IHSRMs.

The sum of stochastic errors of variance and that of cross-covariance are investigated, and the results are pictured in Figures 11 and 12, respectively, to further compare

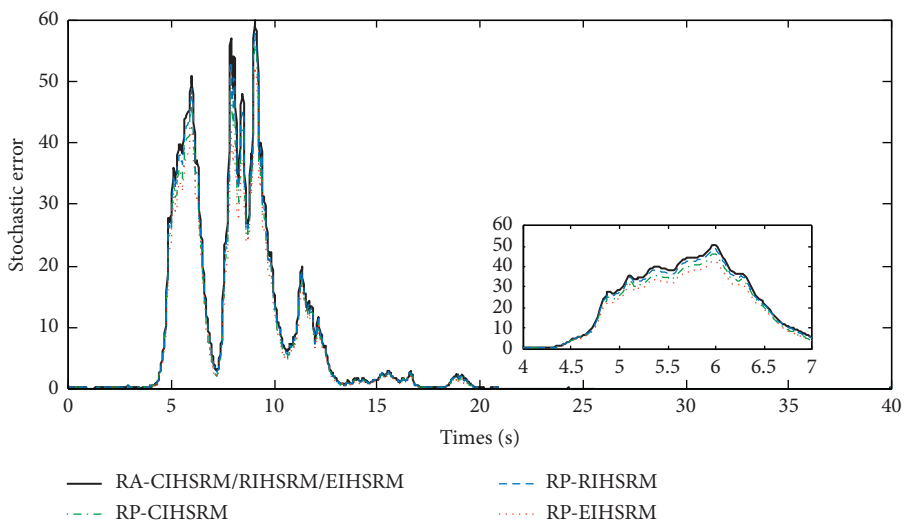

Figure 12: Sum of the stochastic errors of cross-covariance for different methods.

the stochastic errors of covariance for the six types of IHSRMs. As can be seen, the sum values of the variance stochastic errors for RP-IHSRMs are approximately the same. However, taking only the RP-IHSRMs into consideration, the sum value of the stochastic error of cross-covariance for the RP-RIHSRM is the largest, while that for the RP-EIHSRM is the lowest, despite that the differences are slight.

5. Conclusion

A random phase-based IHSRM is proposed to facilitate the simulation of SCEGMs possessing the nonstationary characteristics of the natural record, and a series of deduction and one numerical example are used to verify the validness of the proposed method. Besides, this paper presents an error assessment for the IHSRM. The closed-form solutions of predefined statistic errors were derived for the temporal mean, variance, and cross-covariance of the process simulated by six types of IHSRMs. The validness of the derived closed-form statistic errors was proven by a set of comparisons. The error analyses showed that the proposed method is not ergodic. The stochastic errors of temporal covariance produced by RP-IHSRMs are dependent on the matrix decomposition method, while those produced by the RA-IHSRMs are not. The RA-IHSRMs possess higher stochastic errors of temporal covariance than the RP-IHSRMs. Among RP-IHSRMs, the RP-EIHSRM exhibits the smallest stochastic error, while the RP-RIHSRM possesses the largest, but the difference is slight.

Appendix

A. Relation between the Ensemble Averages of the Mean, Variance, and Hilbert Spectrum of the Generated Ground Motions and Those of the Target

The ensemble averages of the mean and variance of $x_m(t)$ and $x_{m,j}(t)$ can be calculated using

$$\mu_m(t) = E[x_m(t)] = E\left\{\mathrm{Re}\left\{\sum_{k=1}^{L}\sum_{j=1}^{N} A_{km,j}(t)e^{i\left[\theta_j(t)+\Phi_{km,j}+\varphi_{k,j}\right]}\right\}\right\} + r(t) = r(t), \tag{A.1}$$

$$\begin{aligned}\sigma_m^2(t) &= E\left\{\left[x_m(t) - r(t)\right]^2\right\} \\ &= E\left\{\sum_{k=1}^{L}\sum_{j=1}^{N} A_{km,j}^2(t)\cos^2\left[\theta_j(t) + \Phi_{km,j} + \varphi_{k,j}\right]\right\} \\ &= \frac{1}{2}\sum_{k=1}^{L}\sum_{j=1}^{N} A_{km,j}^2(t) = \sum_{k=1}^{L}\sum_{j=1}^{N}\sigma_j^2(t)D_{km,j}^2 = \frac{1}{2}\sum_{j=1}^{N} a_j^2(t),\end{aligned} \tag{A.2}$$

$$\mu_{m,j}(t) = E\left[x_{m,j}(t)\right] = \mathrm{Re}\left\{\sum_{k=1}^{L} A_{km,j}(t)e^{i\left[\theta_j(t)+\Phi_{km,j}\right]}E\left[e^{i\varphi_{k,j}}\right]\right\} = 0, \tag{A.3}$$

$$\begin{aligned}\sigma_{m,j}^2(t) &= \mathrm{Var}\left[x_{m,j}(t)\right] \\ &= \sum_{k=1}^{L} A_{km,j}^2(t)\cos^2\left[\theta_j(t) + \Phi_{km,j} + \varphi_{k,j}\right] \\ &= \frac{1}{2}\sum_{k=1}^{L} A_{km,j}^2(t) = \sigma_j^2(t)\sum_{k=1}^{L} D_{km,j}^2 = \sigma_j^2(t)C_{mm,j} = \frac{1}{2}a_j^2(t).\end{aligned} \tag{A.4}$$

Therefore, considering equations (7)–(10), the ensemble averages of the mean and variance of $x_m(t)$ and $x_{m,j}(t)$ are evidently identical with those of the target underlying random process and the jth reference IMF, respectively.

In the present study, the instantaneous frequency of $x_{m,j}(t)$ is still clearly ω_j despite the existence of $\Phi_{km,j}$ and $\varphi_{k,j}$. Furthermore, the square of the amplitude of $\left\{\sum_{k=1}^{L} A_{km,j}(t)e^{i[\theta_j(t)+\Phi_{km,j}+\varphi_{k,j}]}\right\}$ can be expressed as

$$\begin{aligned}\mathrm{Amp}^2 &= \left\{\sum_{k=1}^{L} a_j(t)D_{km,j}\cos\left[\theta_j(t) + \Phi_{km,j} + \varphi_{k,j}\right]\right\}^2 + \left\{\sum_{k=1}^{L} a_j(t)D_{km,j}\sin\left[\theta_j(t) + \Phi_{km,j} + \varphi_{k,j}\right]\right\}^2 \\ &= \sum_{k=1}^{L} a_j^2(t)D_{km,j}^2 + \sum_{p=1}^{L}\sum_{\substack{q=1\\q\neq p}}^{L} a_j^2(t)D_{pm,j}D_{qm,j}\cos\left[\Phi_{pm,j} + \varphi_{p,j} - \Phi_{qm,j} - \varphi_{q,j}\right] \\ &= a_j^2(t)C_{mm,j} + \sum_{p=1}^{L}\sum_{\substack{q=1\\q\neq p}}^{L} a_j^2(t)D_{pm,j}D_{qm,j}\cos\left[\Phi_{pm,j} + \varphi_{p,j} - \Phi_{qm,j} - \varphi_{q,j}\right] \\ &= a_j^2(t) + \sum_{p=1}^{L}\sum_{\substack{q=1\\q\neq p}}^{L} a_j^2(t)D_{pm,j}D_{qm,j}\cos\left[\Phi_{pm,j} + \varphi_{p,j} - \Phi_{qm,j} - \varphi_{q,j}\right].\end{aligned} \tag{A.5}$$

Due to $E(\cos[\varphi_{p,j} - \varphi_{q,j}]) = 0$, the ensemble average of Amp^2 equates to

$$\begin{aligned}E\left(\mathrm{Amp}^2\right) &= a_j^2(t) + \sum_{p=1}^{L}\sum_{\substack{q=1\\q\neq p}}^{L} a_j^2(t)D_{pm,j}D_{qm,j}E\left\{\cos\left[\Phi_{pm,j} + \varphi_{p,j} - \Phi_{qm,j} - \varphi_{q,j}\right]\right\} \\ &= a_j^2(t).\end{aligned} \tag{A.6}$$

Then, the ensemble average of the amplitude of $\left\{\sum_{k=1}^{L} A_{km,j}(t)e^{i[\theta_j(t)+\Phi_{km,j}+\varphi_{k,j}]}\right\}$ is $a_j(t)$, which is equal to the amplitude of the analytical function of the jth target IMF. Therefore, the ensemble average of the Hilbert spectrum of $x_m(t)$

is identical with that of the target underlying random process and, consequently, equates to the Hilbert spectrum of the record.

B. Proof of Equations (34) and (35)

For random phase formulas, the square of the raw estimation of variance of $x_m(t)$ can be expressed as

$$\begin{aligned}\left[\widehat{\sigma}_m^2(t)\right]^2 &= \left\{\left\{\sum_{k1=1}^{L}\sum_{j1=1}^{N} a_{j1}(t)D_{k1m,j1}\cos\left[\theta_{j1}(t)+\varphi_{k1,j1}\right]\right\}\cdot\left\{\sum_{k2=1}^{L}\sum_{j2=1}^{N} a_{j2}(t)D_{k2m,j2}\cos\left[\theta_{k2}(t)+\varphi_{k2,j2}\right]\right\}\right\}^2\\ &= \sum_{k1=1}^{L}\sum_{j1=1}^{N}\sum_{p1=1}^{L}\sum_{q1=1}^{N}\sum_{k2=1}^{L}\sum_{j2=1}^{N}\sum_{p2=1}^{L}\sum_{q2=1}^{N} a_{j1}(t)a_{j2}(t)a_{q1}(t)a_{q2}(t)\cdot D_{k1m,j1}D_{p1m,q1}D_{k2m,j2}D_{p2m,q2}\cdot\cos\left[\theta_{j1}(t)+\varphi_{k1,j1}\right]\\ &\quad\cos\left[\theta_{q1}(t)+\varphi_{p1,q1}\right]\cos\left[\theta_{j2}(t)+\varphi_{k2,j2}\right]\cos\left[\theta_{q2}(t)+\varphi_{p2,q2}\right].\end{aligned} \tag{B.1}$$

If $k1 = p1 = k2 = p2 = k$ and $j1 = q1 = j2 = q2 = j$,

$$E\left[\widehat{\sigma}_m^2(t)\right]^2 = \sum_{k=1}^{L}\sum_{j=1}^{N}\frac{3}{8}a_j^4(t)D_{km,j}^4. \tag{B.2}$$

If $k1 = p1 = k \neq k2 = p2 = p$ and $j1 = q1 = j \neq j2 = q2 = q$ or $k1 = k2 = k \neq p1 = p2 = p$ and $j1 = j2 = j \neq q1 = q2 = q$ or $k1 = p2 = k \neq k2 = p1 = p$ and $j1 = q2 = j \neq j2 = q1 = q$,

$$E\left[\widehat{\sigma}_m^2(t)\right]^2 = \sum_{k=1}^{L}\sum_{j=1}^{N}\sum_{\substack{p=1\\p\neq k}}^{L}\sum_{\substack{q=1\\q\neq j}}^{N}\frac{1}{4}a_j^2(t)a_q^2(t)D_{km,j}^2D_{pm,q}^2. \tag{B.3}$$

Therefore, synthesizing equations (30), (A.2), and (B.1)–(B.3) will yield equation (34). By using the same derivation process, the proof of equation (35) can be conducted by

$$\begin{aligned}\left[\widehat{\sigma}_m^2(t)\right]^2 &= \left\{\left\{\sum_{k1=1}^{L}\sum_{j1=1}^{N}\sigma_{j1}(t)D_{k1m,j1}\left\{A_{k1j1}\cos\left[\theta_{j1}(t)\right]+B_{k1j1}\sin\left[\theta_{j1}(t)\right]\right\}+r(t)\right\}\right.\\ &\quad\left.\cdot\left\{\sum_{k2=1}^{L}\sum_{j2=1}^{N}\sigma_{j2}(t)D_{k2m,j2}\left\{A_{k2j2}\cos\left[\theta_{j2}(t)\right]+B_{k2j2}\sin\left[\theta_{j2}(t)\right]\right\}+r(t)\right\}\right\}^2\\ &= \sum_{k1=1}^{L}\sum_{j1=1}^{N}\sum_{p1=1}^{L}\sum_{q1=1}^{N}\sum_{k2=1}^{L}\sum_{j2=1}^{N}\sum_{p2=1}^{L}\sum_{q2=1}^{N}\sigma_{j1}(t)\sigma_{j2}(t)\sigma_{q1}(t)\sigma_{q2}(t)\cdot D_{k1m,j1}D_{p1m,q1}D_{k2m,j2}D_{p2m,q2}\\ &\quad\cdot\left\{A_{k1j1}\cos\left[\theta_{j1}(t)\right]+B_{k1j1}\sin\left[\theta_{j1}(t)\right]\right\}\cdot\left\{A_{p1q1}\cos\left[\theta_{q1}(t)\right]+B_{p1q1}\sin\left[\theta_{q1}(t)\right]\right\}\\ &\quad\cdot\left\{A_{k2j2}\cos\left[\theta_{j2}(t)\right]+B_{k2j2}\sin\left[\theta_{j2}(t)\right]\right\}\cdot\left\{A_{p2q2}\cos\left[\theta_{q2}(t)\right]+B_{p2q2}\sin\left[\theta_{q2}(t)\right]\right\}.\end{aligned} \tag{B.4}$$

If $k1 = p1 = k2 = p2 = k$ and $j1 = q1 = j2 = q2 = j$,

$$E\left[\widehat{\sigma}_m^2(t)\right]^2 = \sum_{k=1}^{L}\sum_{j=1}^{N}\frac{3}{4}a_j^4(t)D_{km,j}^4. \tag{B.5}$$

If $k1 = p1 = k \neq k2 = p2 = p$ and $j1 = q1 = j \neq j2 = q2 = q$ or $k1 = k2 = k \neq p1 = p2 = p$ and $j1 = j2 = j \neq q1 = q2 = q$ or $k1 = p2 = k \neq k2 = p1 = p$ and $j1 = q2 = j \neq j2 = q1 = q$,

$$E\left[\widehat{\sigma}_m^2(t)\right]^2 = \sum_{k=1}^{L}\sum_{j=1}^{N}\sum_{\substack{p=1\\p\neq k}}^{L}\sum_{\substack{q=1\\q\neq j}}^{N}\frac{1}{4}a_j^2(t)a_q^2(t)D_{km,j}^2D_{pm,q}^2. \tag{B.6}$$

Therefore, synthesizing equations (30) and (B.4)–(B.6) will yield equation (35).

C. Proof of Equations (41) and (42)

For random phase formulas, the square of the raw estimation of cross-covariance between $x_m(t)$ and $x_n(t)$ can be expressed as

$$\begin{aligned}\left[\widehat{\mathrm{COV}}_{mn}(t)\right]^2 &= \left\{\left\{\sum_{k1=1}^{L}\sum_{j1=1}^{N} a_{j1}(t)D_{k1m,j1}\cos\left[\theta_{j1}(t)+\varphi_{k1,j1}\right]\right\}\cdot\left\{\sum_{k2=1}^{L}\sum_{j2=1}^{N} a_{j2}(t)D_{k2n,j2}\cos\left[\theta_{j2}(t)+\varphi_{k2,j2}\right]\right\}\right\}^2\\ &= \sum_{k1=1}^{L}\sum_{j1=1}^{N}\sum_{p1=1}^{L}\sum_{q1=1}^{N}\sum_{k2=1}^{L}\sum_{j2=1}^{N}\sum_{p2=1}^{L}\sum_{q2=1}^{N} a_{j1}(t)a_{q1}(t)a_{j2}(t)a_{q2}(t)\cdot D_{k1m,j1}D_{p1n,q1}D_{k2m,j2}D_{p2n,q2}\cdot\cos\left[\theta_{j1}(t)+\varphi_{k1,j1}\right]\\ &\quad\cdot\cos\left[\theta_{q1}(t)+\varphi_{p1,q1}\right]\cdot\cos\left[\theta_{j2}(t)+\varphi_{k2,j2}\right]\cos\left[\theta_{q2}(t)+\varphi_{p2,q2}\right].\end{aligned} \tag{C.1}$$

If $k1 = p1 = k2 = p2 = k$ and $j1 = q1 = j2 = q2 = j$,

$$E\left[\widehat{\mathrm{COV}}_{mn}(t)\right]^2 = \sum_{k=1}^{L}\sum_{j=1}^{N}\frac{3}{8}a_j^4(t)D_{km,j}^2D_{kn,j}^2. \tag{C.2}$$

If $k1 = p1 = k \neq k2 = p2 = p$ and $j1 = q1 = j \neq j2 = q2 = q$ or $k1 = p2 = k \neq k2 = p1 = p$ and $j1 = q2 = j \neq j2 = q1 = q$,

$$E\left[\widehat{\mathrm{COV}}_{mn}(t)\right]^2 = \sum_{k=1}^{L}\sum_{j=1}^{N}\sum_{\substack{p=1\\p\neq k}}^{L}\sum_{\substack{q=1\\q\neq j}}^{N}\frac{1}{4}a_j^2(t)a_q^2(t)D_{km,j}D_{kn,j}D_{pm,q}D_{pn,q}. \tag{C.3}$$

If $k1 = k2 = k \neq p1 = p2 = p$ and $j1 = j2 = j \neq q1 = q2 = q$,

$$E\left[\widehat{\mathrm{COV}}_{mn}(t)\right]^2 = \sum_{k=1}^{L}\sum_{j=1}^{N}\sum_{\substack{p=1\\p\neq k}}^{L}\sum_{\substack{q=1\\q\neq j}}^{N}\frac{1}{4}a_j^2(t)a_q^2(t)D_{km,j}^2D_{pn,q}^2. \tag{C.4}$$

Therefore, synthesizing equations (30), (38), and (C.1)–(C.4) will yield equation (41).

For random amplitude formulas,

$$\begin{aligned}\left[\widehat{\mathrm{COV}}_{mn}(t)\right]^2 &= \left\{\left\{\sum_{k1=1}^{L}\sum_{j1=1}^{N}\sigma_{j1}(t)D_{k1m,j1}\left\{A_{k1j1}\cos\left[\theta_{j1}(t)\right]+B_{k1j1}\sin\left[\theta_{j1}(t)\right]\right\}+r(t)\right\}\right.\\ &\quad\left.\cdot\left\{\sum_{k2=1}^{L}\sum_{j2=1}^{N}\sigma_{j2}(t)D_{k2n,j2}\left\{A_{k2j2}\cos\left[\theta_{j2}(t)\right]+B_{k2j2}\sin\left[\theta_{j2}(t)\right]\right\}+r(t)\right\}\right\}^2\\ &= \sum_{k1=1}^{L}\sum_{j1=1}^{N}\sum_{p1=1}^{L}\sum_{q1=1}^{N}\sum_{k2=1}^{L}\sum_{j2=1}^{N}\sum_{p2=1}^{L}\sum_{q2=1}^{N}\sigma_{j1}(t)\sigma_{j2}(t)\sigma_{q1}(t)\sigma_{q2}(t)\cdot D_{k1m,j1}D_{p1n,q1}D_{k2m,j2}D_{p2n,q2}\\ &\quad\cdot\left\{A_{k1j1}\cos\left[\theta_{j1}(t)\right]+B_{k1j1}\sin\left[\theta_{j1}(t)\right]\right\}\cdot\left\{A_{p1q1}\cos\left[\theta_{q1}(t)\right]+B_{p1q1}\sin\left[\theta_{q1}(t)\right]\right\}\\ &\quad\cdot\left\{A_{k2j2}\cos\left[\theta_{j2}(t)\right]+B_{k2j2}\sin\left[\theta_{j2}(t)\right]\right\}\cdot\left\{A_{p2q2}\cos\left[\theta_{q2}(t)\right]+B_{p2q2}\sin\left[\theta_{q2}(t)\right]\right\}.\end{aligned} \tag{C.5}$$

If $k1 = p1 = k2 = p2 = k$ and $j1 = q1 = j2 = q2 = j$,

$$E\left[\widehat{\mathrm{COV}}_{mn}(t)\right]^2 = \sum_{k=1}^{L}\sum_{j=1}^{N}\frac{3}{4}a_j^4(t)D_{km,j}^2D_{kn,j}^2. \tag{C.6}$$

If $k1 = p1 = k \neq k2 = p2 = p$ and $j1 = q1 = j \neq j2 = q2 = q$ or $k1 = p2 = k \neq k2 = p1 = p$ and $j1 = q2 = j \neq j2 = q1 = q$,

$$E\left[\widehat{\mathrm{COV}}_{mn}(t)\right]^2 = \sum_{k=1}^{L}\sum_{j=1}^{N}\sum_{\substack{p=1\\p\neq k}}^{L}\sum_{\substack{q=1\\q\neq j}}^{N}\frac{1}{4}a_j^2(t)a_q^2(t)D_{km,j}D_{kn,j}D_{pm,q}D_{pn,q}. \tag{C.7}$$

If $k1 = k2 = k \neq p1 = p2 = p$ and $j1 = j2 = j \neq q1 = q2 = q$,

$$E\left[\widehat{\mathrm{COV}}_{mn}(t)\right]^2 = \sum_{k=1}^{L}\sum_{j=1}^{N}\sum_{\substack{p=1\\p\neq k}}^{L}\sum_{\substack{q=1\\q\neq j}}^{N}\frac{1}{4}a_j^2(t)a_q^2(t)D_{km,j}^2D_{pn,q}^2. \tag{C.8}$$

Therefore, synthesizing equations (30), (39), and (C.5)–(C.8) will yield equation (42).

Data Availability

All the data supporting the conclusions of this study are presented in the figures and tables of the article. The code and details involved in this paper are available upon request from the corresponding author.

Conflicts of Interest

The authors declare that there are no conflicts of interest regarding the publication of this paper.

Acknowledgments

This study was financially supported by the National Natural Science Foundation of China (no. 51908236), the China Postdoctoral Science Foundation (2019M652649), and the Basic Operating Expenses of the Central Level Public Welfare Research Institutes (CKSF2019193/YT and CKSF2019477/YT).

References

[1] S. O. Rice, *Mathematical Analysis of Random Noise. Selected Papers on Noise and Stochastic Processes*, Dover Publications., New York, NY, USA, 1954.

[2] M. Shinozuka, "Simulation of multivariate and multidimensional random processes," *The Journal of the Acoustical Society of America*, vol. 49, no. 1B, pp. 357–368, 1971.

[3] M. Shinozuka, "Monte Carlo solution of structural dynamics," *Computers and Structures*, vol. 2, no. 5-6, pp. 855–874, 1972.

[4] M. Shinozuka and C.-M. Jan, "Digital simulation of random processes and its applications," *Journal of Sound and Vibration*, vol. 25, no. 1, pp. 111–128, 1972.

[5] G. Huang, "An efficient simulation approach for multivariate nonstationary process: hybrid of wavelet and spectral representation method," *Probabilistic Engineering Mechanics*, vol. 37, no. 10, pp. 74–83, 2014.

[6] J. Liang, S. R. Chaudhuri, and M. Shinozuka, "Simulation of nonstationary stochastic processes by spectral representation," *Journal of Engineering Mechanics*, vol. 133, no. 6, pp. 616–627, 2007.

[7] Y. Gao, Y. Wu, D. Li, Y. Cai, H. Liu, and N. Zhang, "Error assessment for the coherency matrix-based spectral representation method in multivariate random processes simulation," *Journal of Engineering Mechanics*, vol. 139, no. 9, pp. 1294–1299, 2013.

[8] J. Liang, Z. Liu, L. Huang, and G. Yang, "The indirect boundary integral equation method for the broadband scattering of plane P, SV and Rayleigh waves by a hill topography," *Engineering Analysis with Boundary Elements*, vol. 98, pp. 184–202, 2019.

[9] L. Huang, Z. Liu, C. Wu, and J. Liang, "The scattering of plane P, SV waves by twin lining tunnels with imperfect interfaces embedded in an elastic half-space," *Tunnelling and Underground Space Technology*, vol. 85, pp. 319–330, 2019.

[10] E. Yao, Y. Miao, S. Wang, and X. Long, "Simulation of fully nonstationary spatially variable ground motions on a canyon site," *Soil Dynamics and Earthquake Engineering*, vol. 115, pp. 198–204, 2018.

[11] E. Yao, S. Wang, B. Ruan, Y. Miao, and L. Zhu, "Numerical study on site response considering ground motion spatial variation," *Soil Dynamics and Earthquake Engineering*, vol. 127, Article ID 105836, 2019.

[12] E. Yao, S. Wang, Y. Miao, L. Ye, and L. Zhu, "Simulation of fully non-stationary spatially varying ground motions considering nonlinear soil behavior," *Soil Dynamics and Earthquake Engineering*, vol. 129, Article ID 105954, 2020.

[13] L. Hu, L. Li, and M. Gu, "Error assessment for spectral representation method in wind velocity field simulation," *Journal of Engineering Mechanics*, vol. 136, no. 9, pp. 1090–1104, 2010.

[14] Y. Gao, Y. Wu, Y. Cai, H. Liu, D. Li, and N. Zhang, "Error assessment for spectral representation method in random field simulation," *Journal of Engineering Mechanics*, vol. 138, no. 6, pp. 711–715, 2012.

[15] L. Hu, Z. F. Xu, Y. L. Xu et al., "Error analysis of spatially varying seismic ground motion simulation by spectral representation method," *Journal of Engineering Mechanics, ASCE*, vol. 143, no. 9, Article ID 04017083, 2017.

[16] Z. F. Xu, L. Li, and L. Hu, "Estimation of evolutionary spectra of monitored seismic ground motions by transformation of correlation functions," *Shock and Vibration*, vol. 2015, Article ID 846943, 9 pages, 2015.

[17] Y. X. Wu, Y. F. Gao, and D. Y. Li, "Error assessment of multivariate random processes simulated by a conditional-simulation method," *Journal of Engineering Mechanics, ASCE*, vol. 141, no. 5, Article ID 04014155, 2014.

[18] Y. K. Wen and P. Gu, "Description and simulation of nonstationary processes based on Hilbert spectra," *Journal of Engineering Mechanics*, vol. 130, no. 8, pp. 942–951, 2004.

[19] N. E. Huang, Z. Shen, S. R. Long et al., "The empirical mode decomposition and the Hilbert spectrum for nonlinear and non-stationary time series analysis," *Proceedings of the Royal Society of London. Series A: Mathematical, Physical and Engineering Sciences*, vol. 454, no. 1971, pp. 903–995, 1998.

[20] Y. Miao, E. Yao, B. Ruan, H. Zhuang, G. Chen, and X. Long, "Improved hilbert spectral representation method and its application to seismic analysis of shield tunnel subjected to spatially correlated ground motions," *Soil Dynamics and Earthquake Engineering*, vol. 111, pp. 119–130, 2018.

[21] M. Di Paola and M. Zingales, "Digital simulation of multivariate earthquake ground motions," *Earthquake Engineering & Structural Dynamics*, vol. 29, no. 7, pp. 1011–1027, 2000.

[22] H. Hao, C. S. Oliveira, and J. Penzien, "Multiple-station ground motion processing and simulation based on smart-1 array data," *Nuclear Engineering and Design*, vol. 111, no. 3, pp. 293–310, 1989.

[23] Y. X. Wu, Y. F. Gao, N. Zhang et al., "Simulation of spatially varying non–Gaussian and nonstationary seismic ground motions by the spectral representation method," *Journal of Engineering Mechanics, ASCE*, vol. 144, no. 1, Article ID 04017143, 2018.

[24] Y. Wu and Y. Gao, "A modified spectral representation method to simulate non-Gaussian random vector process

considering wave-passage effect," *Engineering Structures*, vol. 201, Article ID 109587, 2019.

[25] Y. Wu, Y. Gao, L. Zhang, and J. Yang, "How the distribution characteristics of soil property affect probabilistic foundation settlement: from the view of the first four statistical moments," *Canadian Geotechnical Journal*, vol. 57, no. 4, pp. 595–607, 2020.

[26] E. H. Vanmarcke and G. A. Fenton, "Conditioned simulation of local fields of earthquake ground motion," *Structural Safety*, vol. 10, no. 1–3, pp. 247–264, 1991.

[27] E. H. Vanmarcke, E. Heredia-Zavoni, and G. A. Fenton, "Conditional simulation of spatially correlated earthquake ground motion," *Journal of Engineering Mechanics*, vol. 119, no. 11, pp. 2333–2352, 1993.

[28] A. Zerva and M. Shinozuka, "Stochastic differential ground motion," *Structural Safety*, vol. 10, no. 1-3, pp. 129–143, 1991.

[29] J. S. Bendat and A. G. Piersol, *Random Data: Analysis and Measurement Procedures*, Wiley, New York, NY, USA, 1986.